Molecular Orientation and Electronic Excitations at Organic Photovoltaic Interfaces

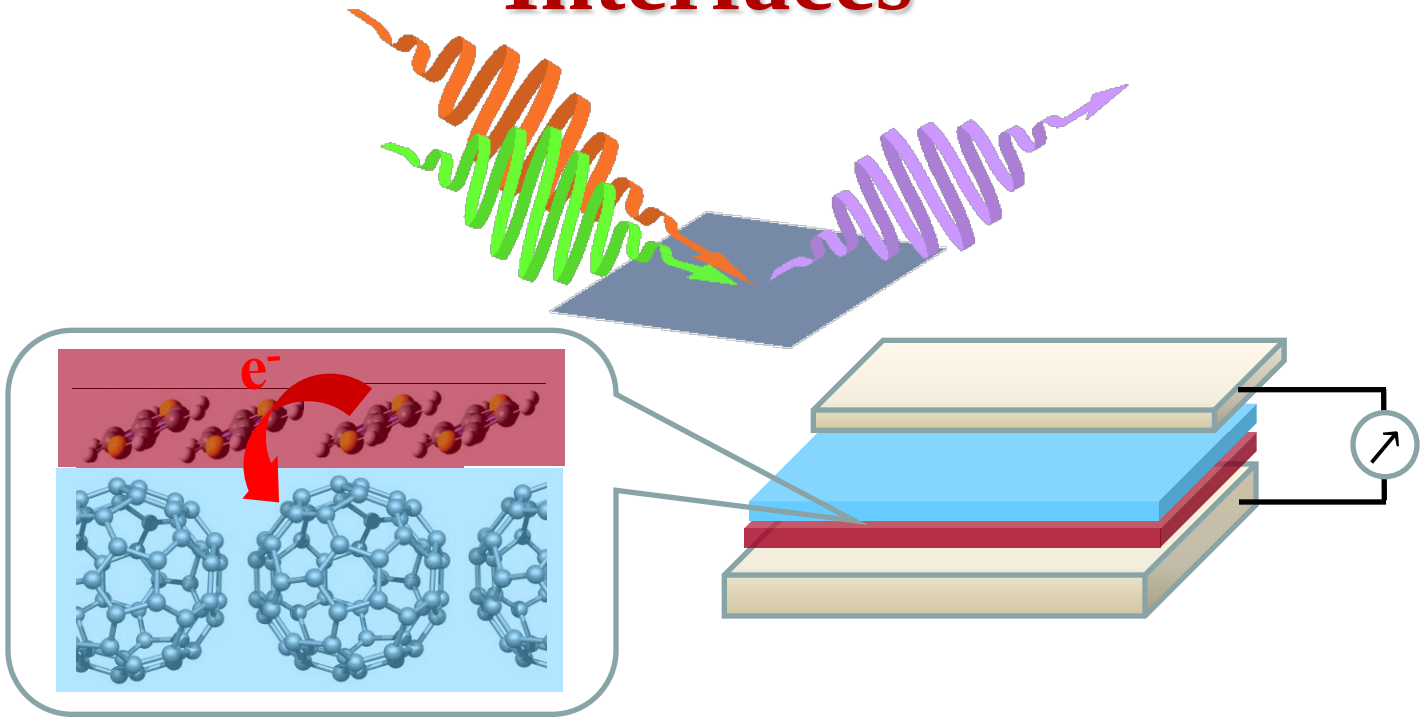

Alex Benderskii
Department of Chemistry
University of Southern California

Research Overview:

Molecular structure and dynamics at surfaces and interfaces

Technique development

HD-SFG

Time-delay effects in line shapes

STiR-SFG

SFG-FID

JACS **130**, 2271 (2008); *JCP* **132**, 234503 (2010); *JPC*B **109**, 15941 (2005); *JCP* **122**, 134713 (2005)

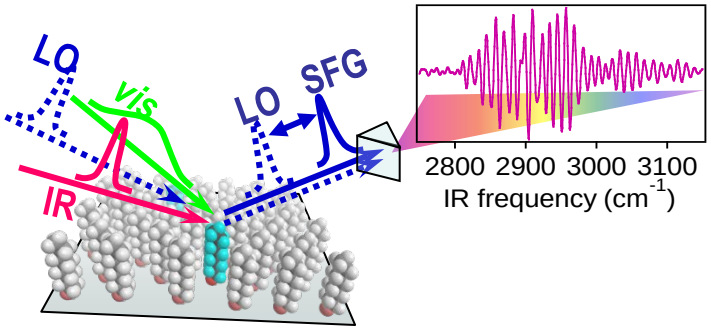

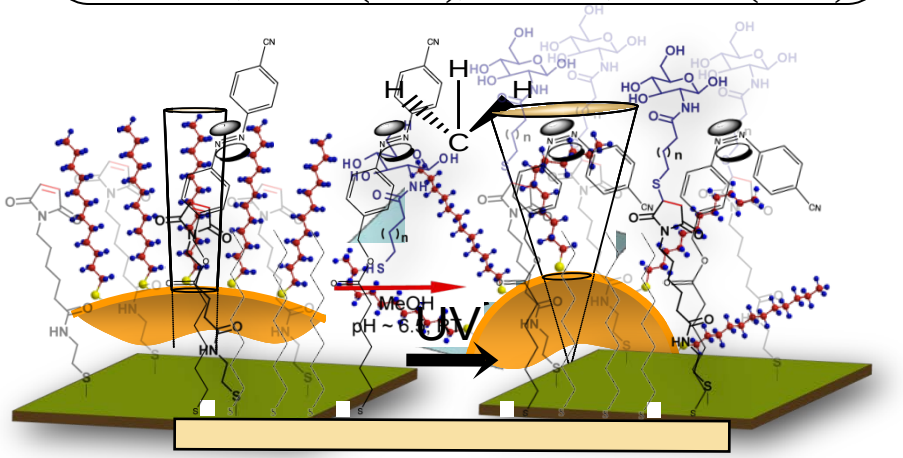

Surfaces of Materials/Nanostructures

Structure, conformation, reactivity

Functionalized & photoactive surfaces

Surface passivation

LB monolayer films

Heterogeneous catalysis

Polymers and OPV

Langmuir **25**, 6880 (2009), *Langmuir* **25**, 1901 (2009); *JPC* C **111**, 8925 (2007) *JACS* **128**, 14244 (2006); *JCP* **125**, 064706 (2006), *JPC C* **117**, 935 (2013), *JPC C* ***117***, 15213 (2013)

Aqueous interfaces

H-bonding

Vibrational dynamics/coupling

Rotational dynamics

Nature **474**, 192 (2011); *JCP* **122**, 134713 (2005), *JPCL* **3**, 3348 (2012), *JPC B* **117**, 15833 (2013)

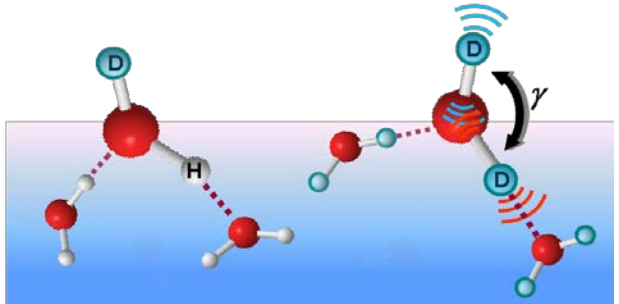

Interfaces in Organic and Hybrid Photovoltaics

- **The donor-acceptor interface:**
  - **Organic-organic**
  - **Organic-inorganic**

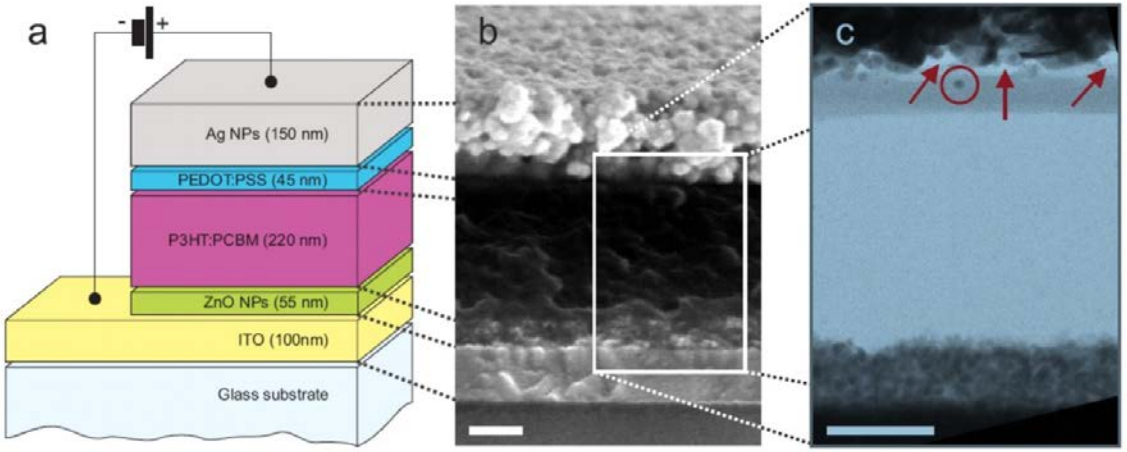

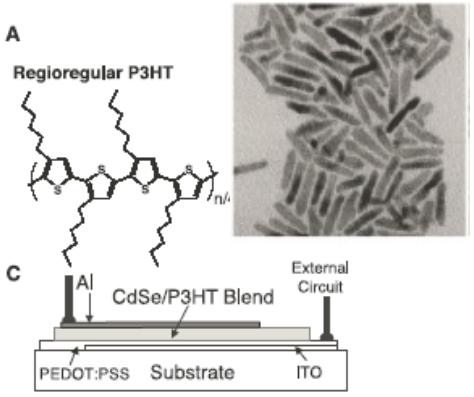

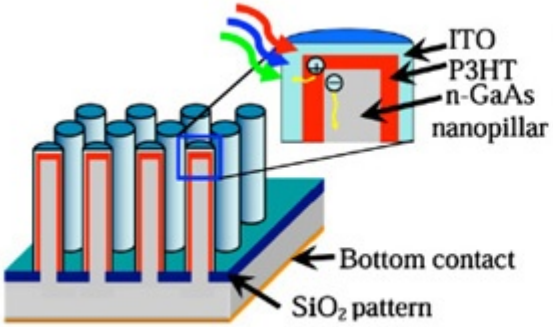

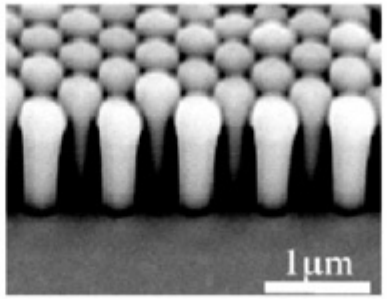

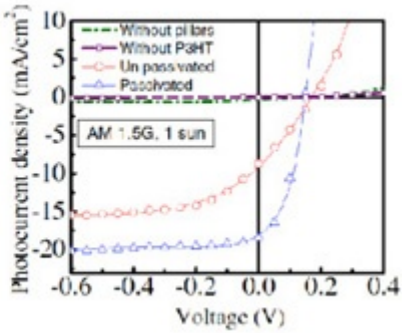

Interfaces in Organic and Hybrid Photovoltaics

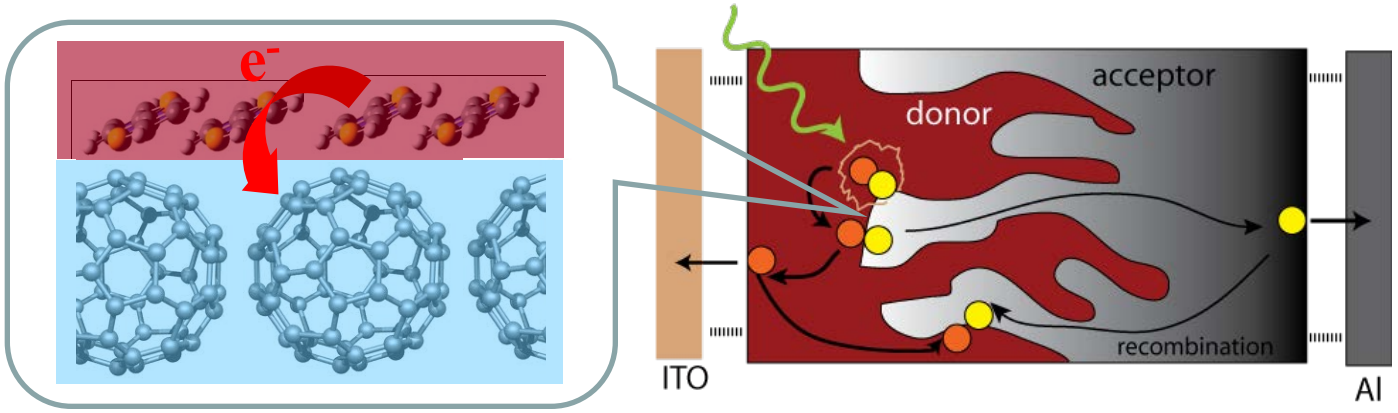

Interfaces in Organic and Hybrid Photovoltaics

Molecular structure:
orientation, conformation
vSFG, MD

Device manufacturing
prep. conditions

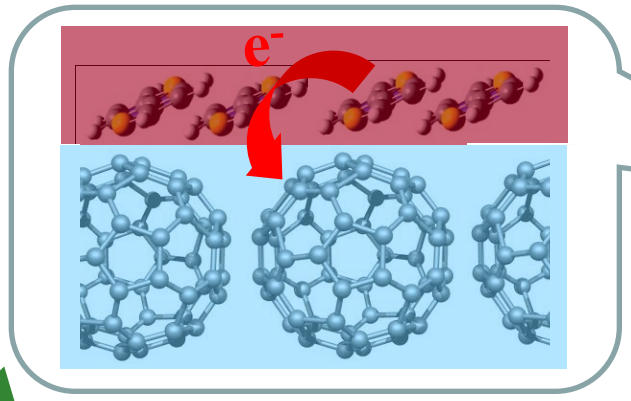

Planar devices

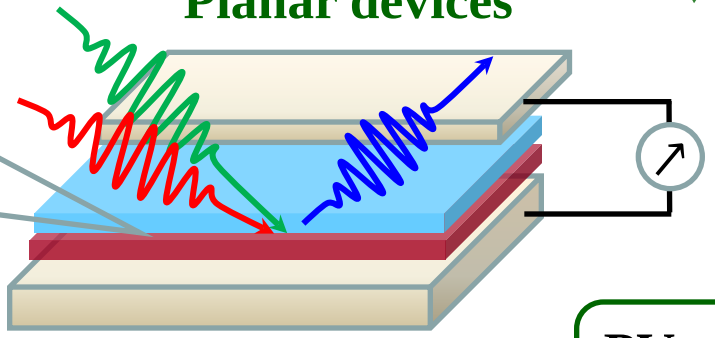

PV efficiency
measurements

Electronic states
eSHG, ab initio (DFT)

ET rate (forward/back)
TR-SHG, NAQMD

Nonlinear laser spectroscopy

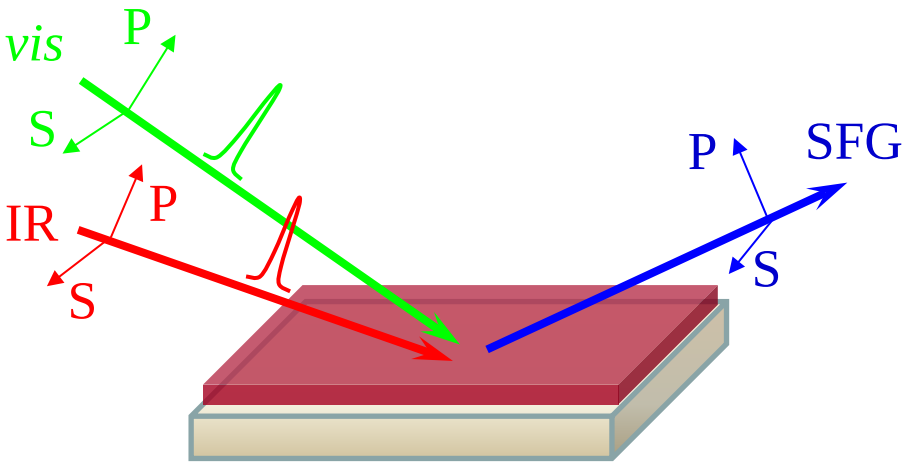

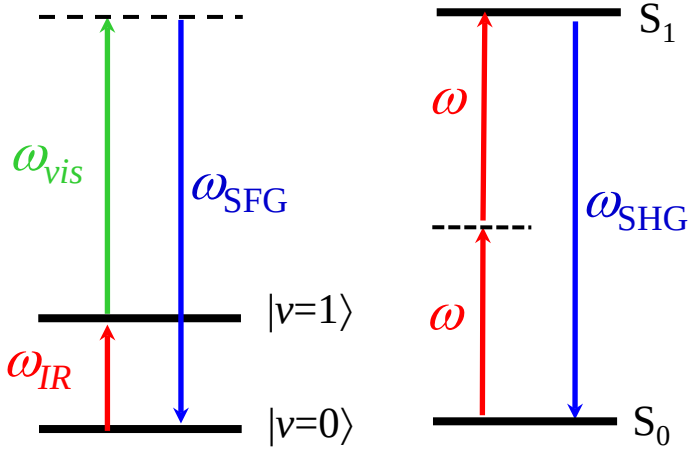

Vibrational Sum Frequency Generation

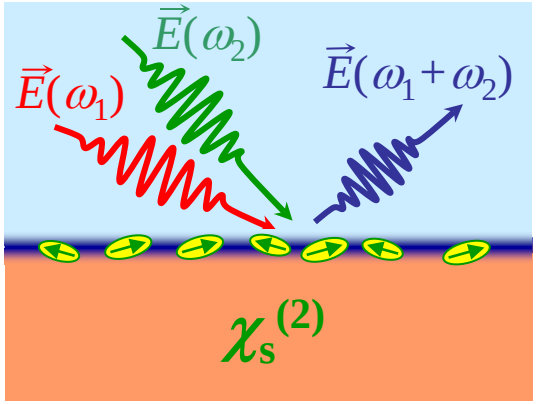

$$E_i(\omega_{SFG}) \propto P_{ijk}^{(2)} = \chi^{(2)}_{ijk}\,(\omega_1,\omega_2)\,E_j(\omega_1)E_k(\omega_2)$$

Molecular origin of $\chi^{(2)}$:

$$\chi^{(2)}_{ijk} = N_s \langle T_{i\lambda} T_{j\mu} T_{k\nu} \rangle_{\theta,\varphi,\psi} \beta_{\lambda\mu\nu}^{(2)}(\omega)$$

SFG signal intensity

Surface coverage

Molecular orientation

Polarization measurements

Spectroscopic selectivity (resonant enhancement)

Time and frequency-domain (line shapes, dephasing dynamics)

Propensity rules (structure, conformation)

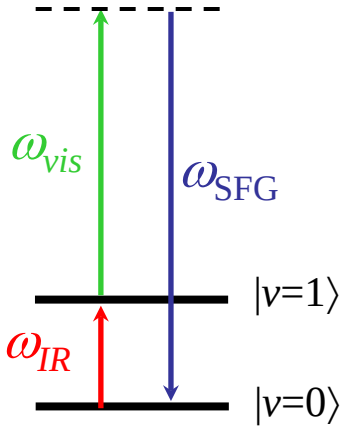

Interfaces in Organic and Hybrid Photovoltaics

Ab initio of CT state

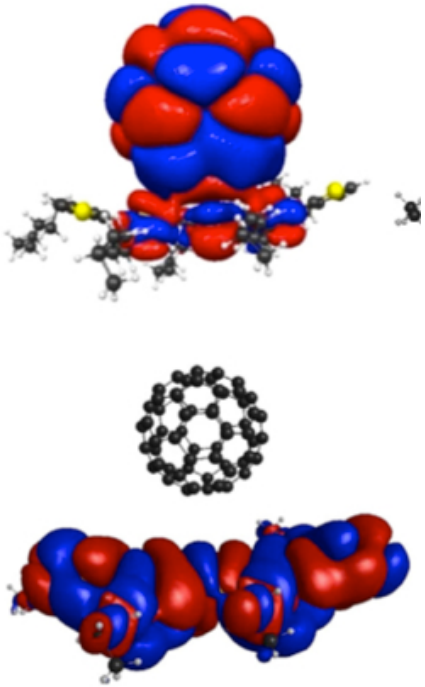

C.F.N. Marchiori, M. Koehler
Syn. Met. 160 (2010) 643–650

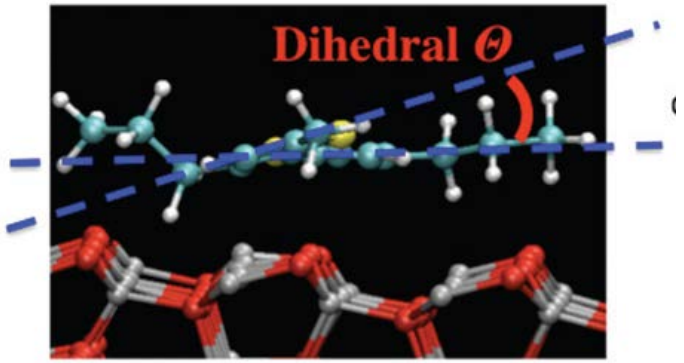

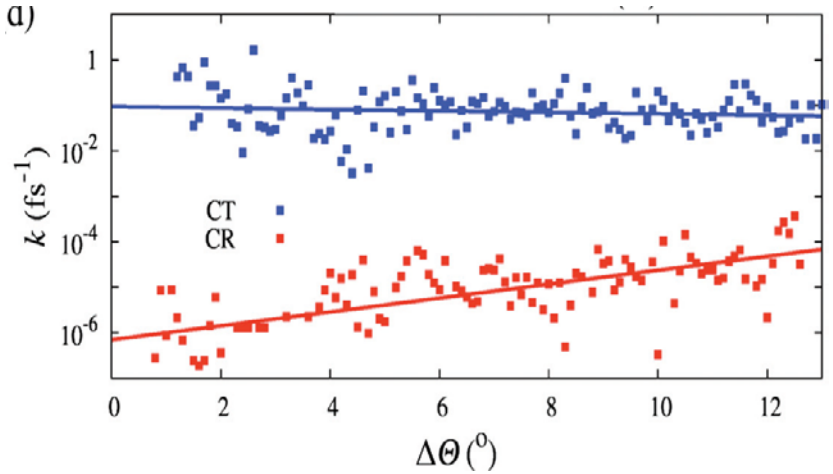

W. Mou, S. Ohmura, F. Shimojo, and A. Nakano *Appl. Phys. Lett.* 100, 203306 (2012)

P3HT vibrational spectroscopy

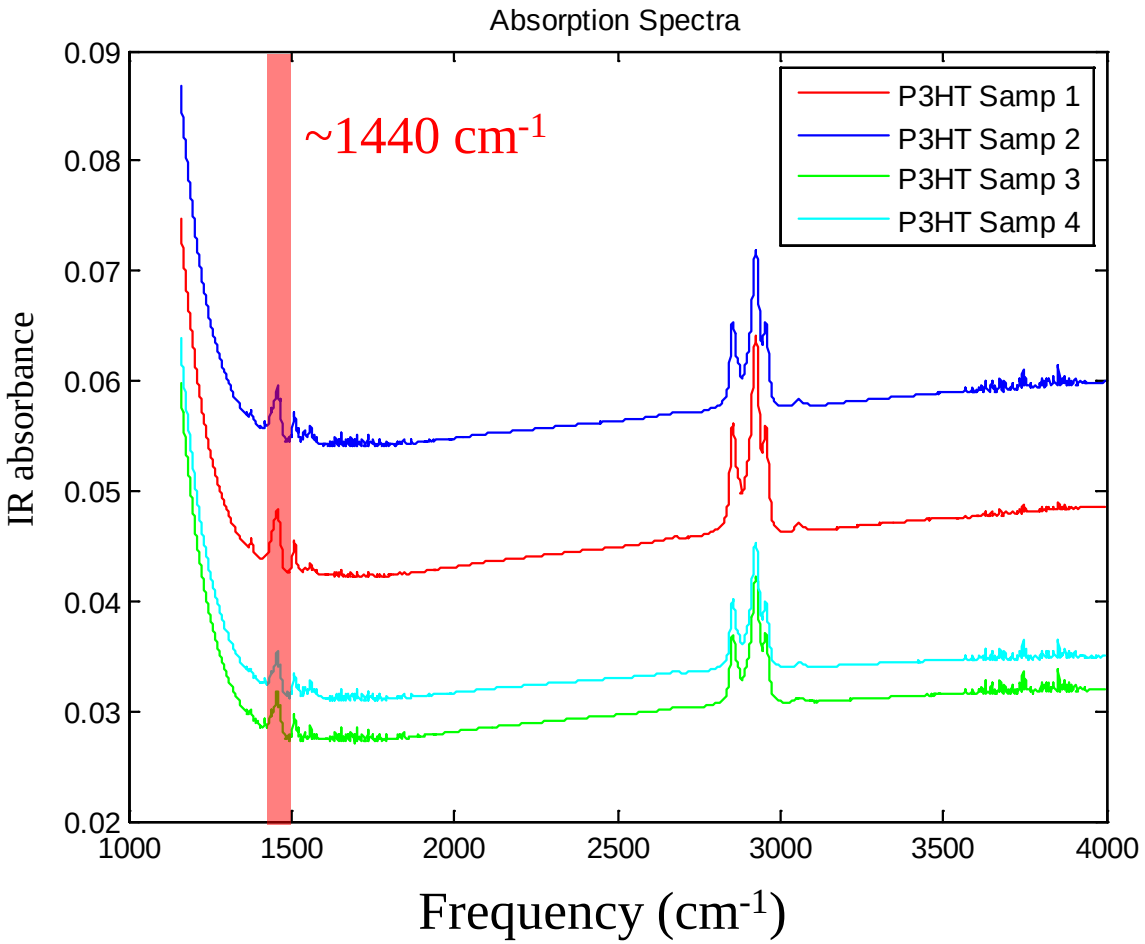

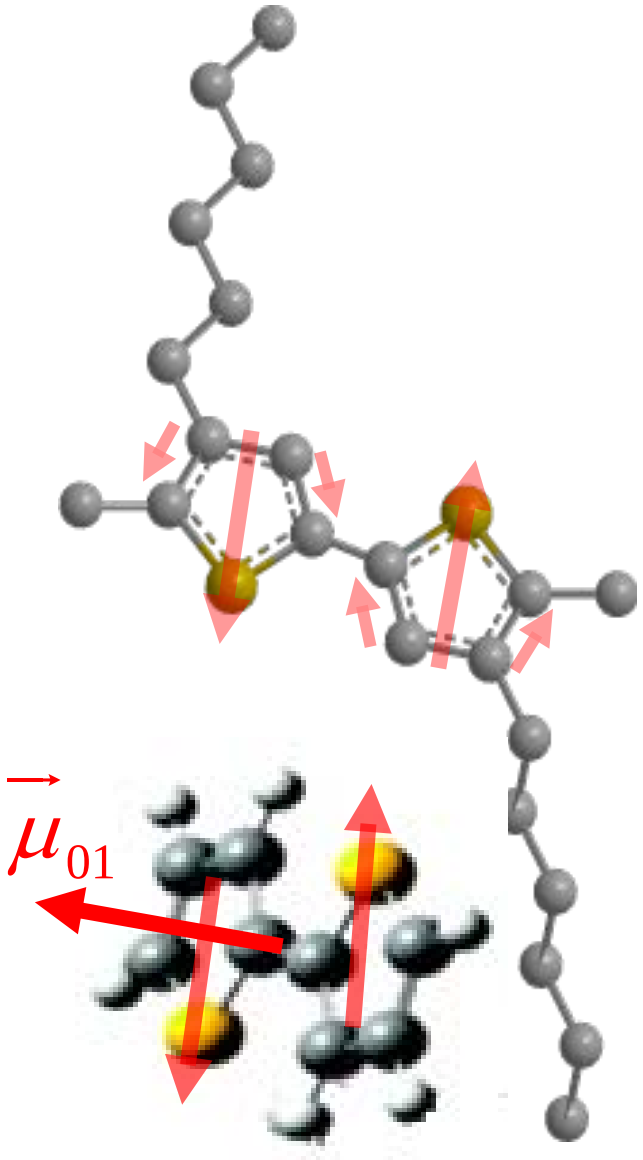

Anglin, Speros, Massari, *JPC C* **2011**, *115*, 16027

Molecular orientation at surfaces by VSFG

IR absorption

NOT surface-selective

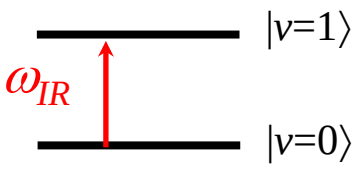

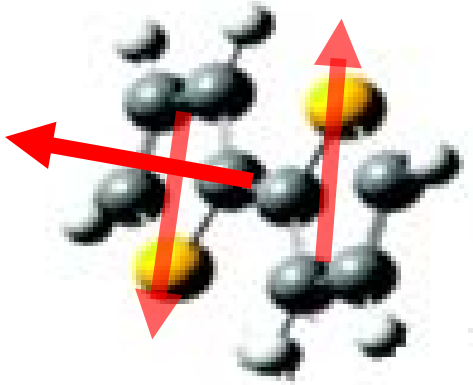

vSFG

surface-selective

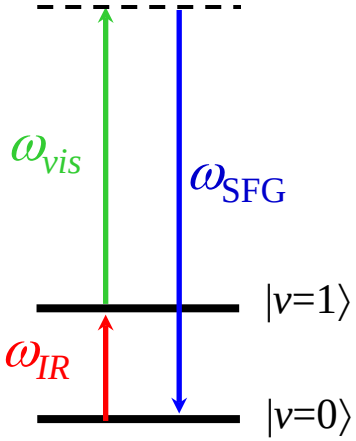

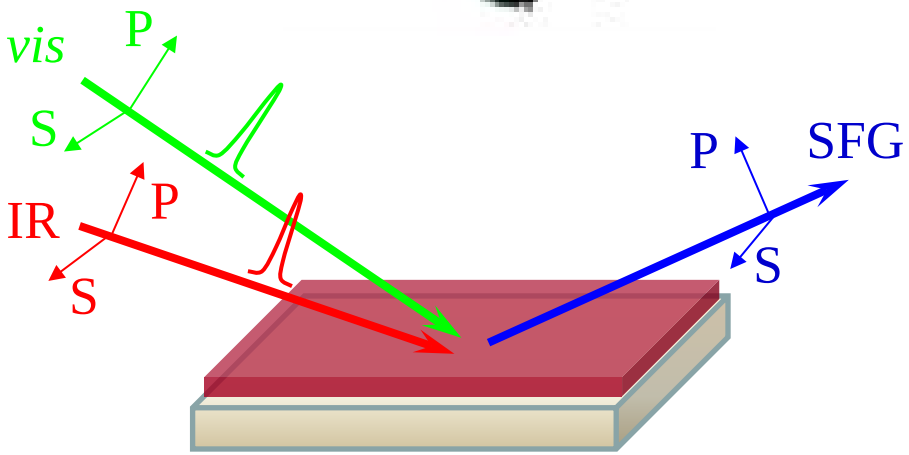

Vibrational SFG spectroscopy of P3HT surface

Effect of annealing: SiO_2 interface

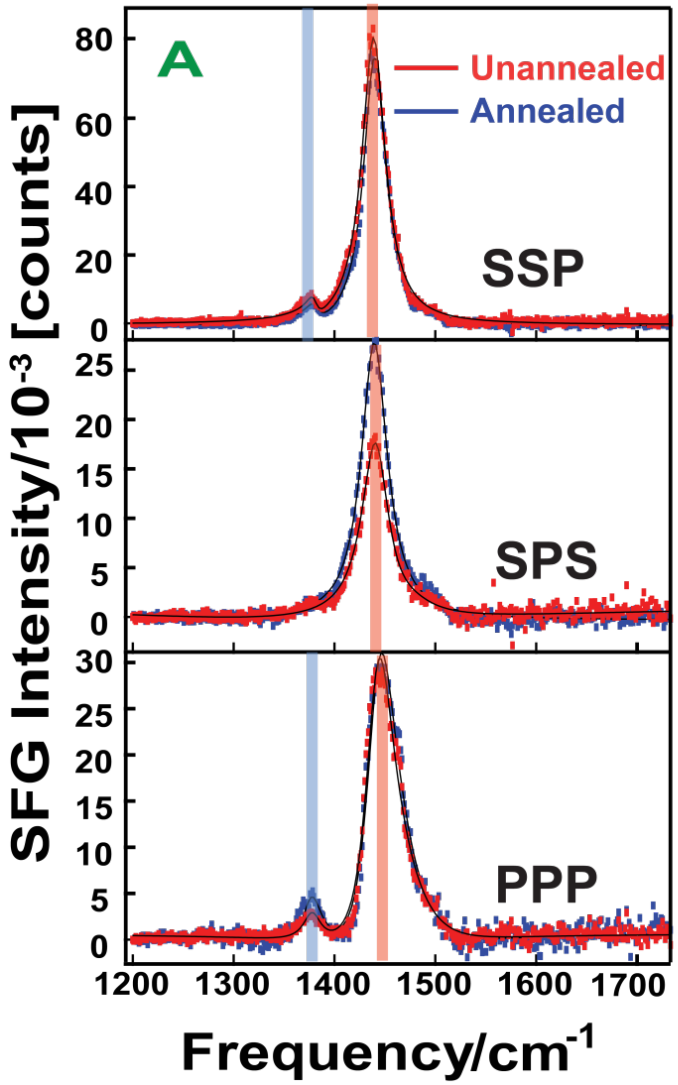

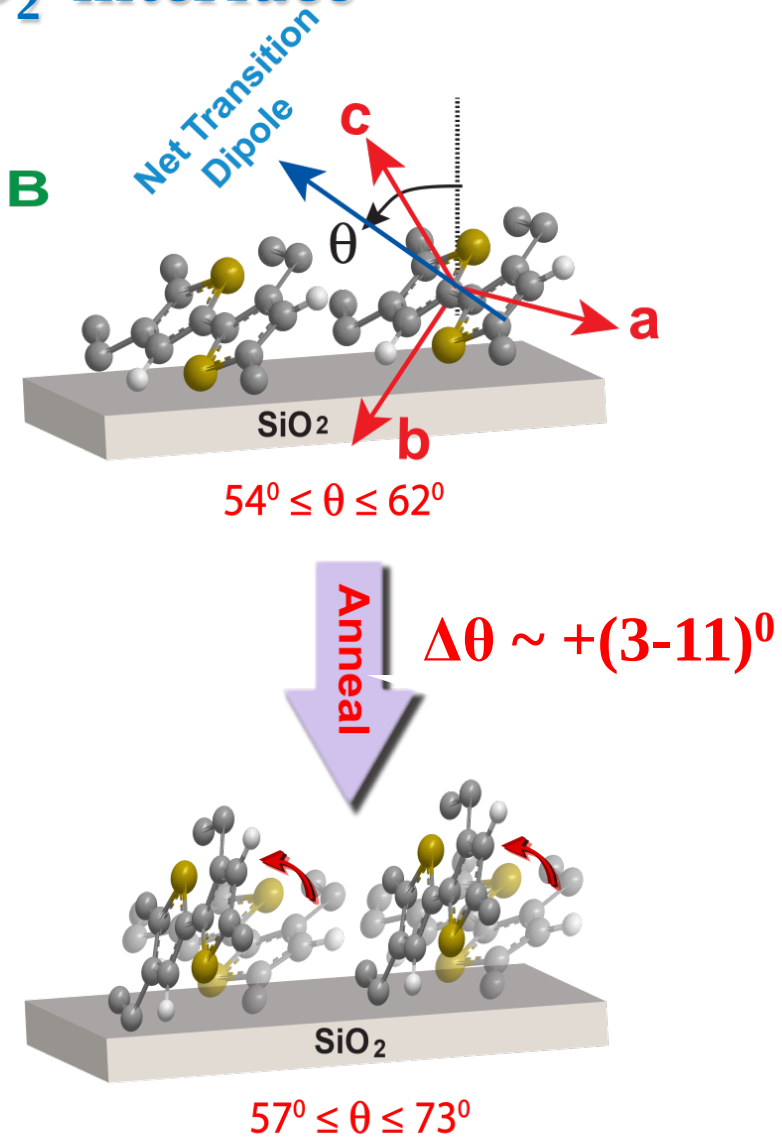

Dhar *et al*. *JPC C* **2013**, *117*, 15213

Vibrational SFG spectroscopy of P3HT surface

Effect of annealing: Al_2O_3 interface

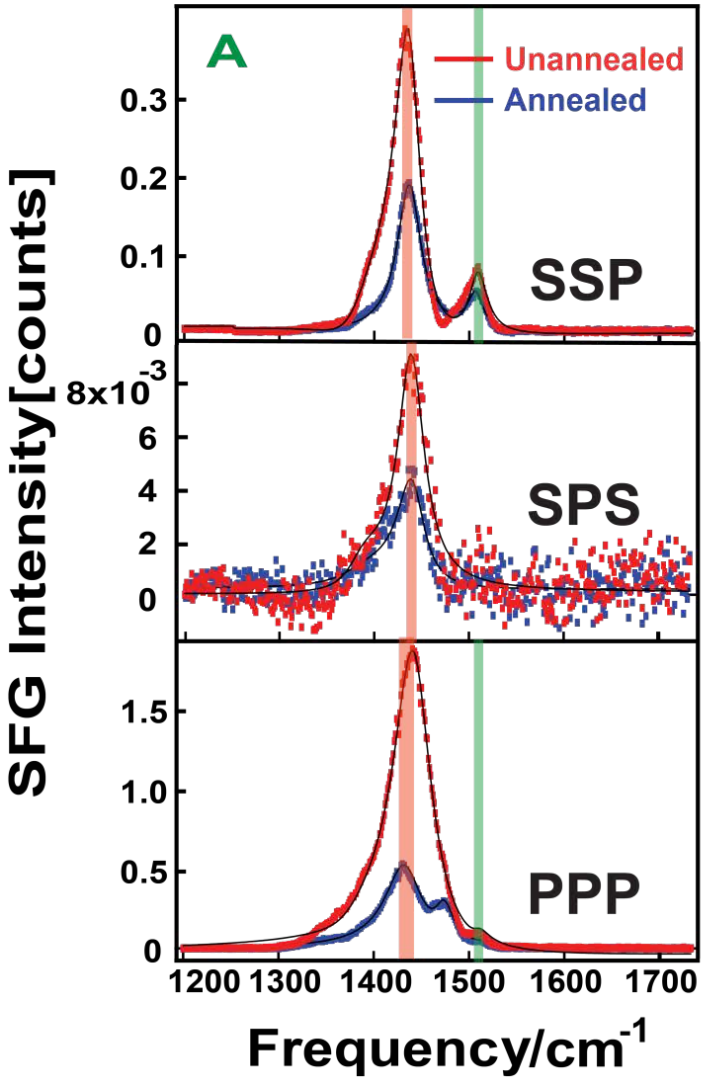

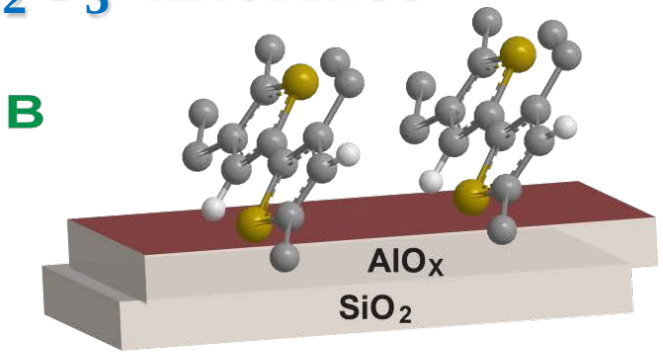

$47^0 \le \theta \le 75^0$

Anneal

$\Delta\theta \sim -(3\text{-}26)^0$

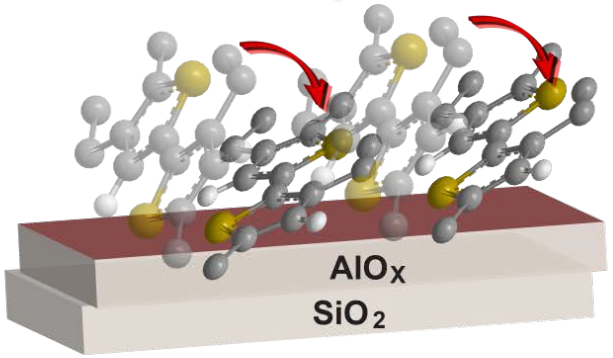

$44^0 \le \theta \le 49^0$

Dhar *et al*. *JPC C* **2013**, *117*, 15213

Electronic states at OPV interfaces

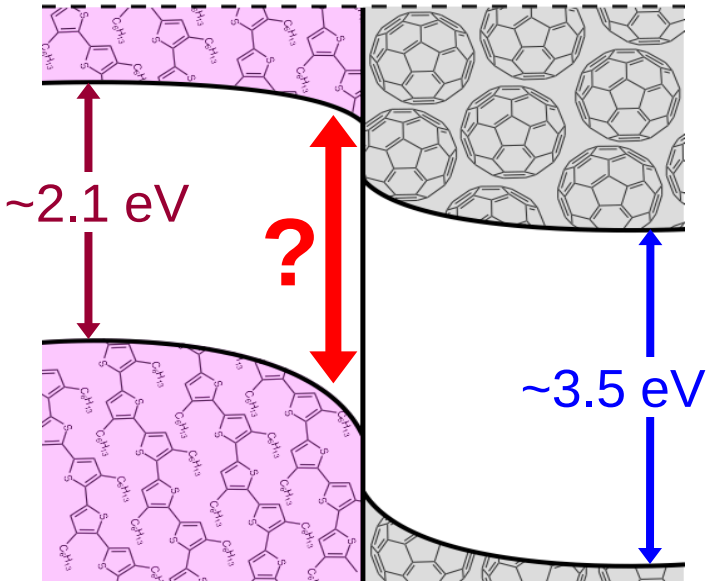

UV-vis absorption
(NOT surface-selective)

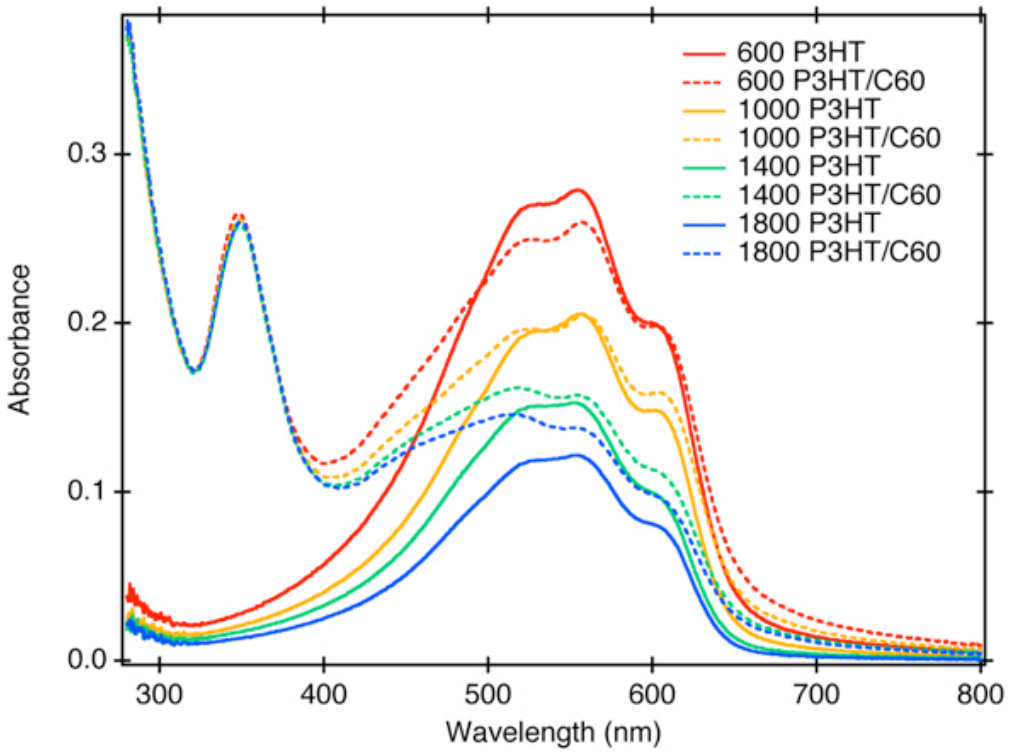

- **Surface partitioning**
- **Polymer conformation**
- **Surface charging**

Generation of narrow-band (ps) 400 nm pulses

Broad-band
800nm
50 fs
400 cm^{-1}

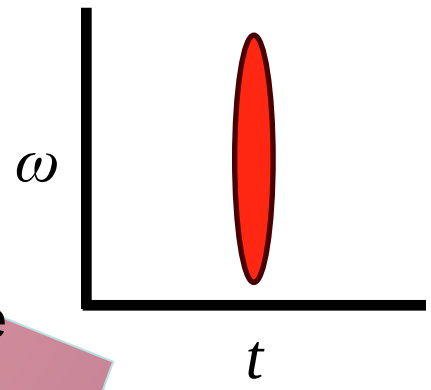

BBO

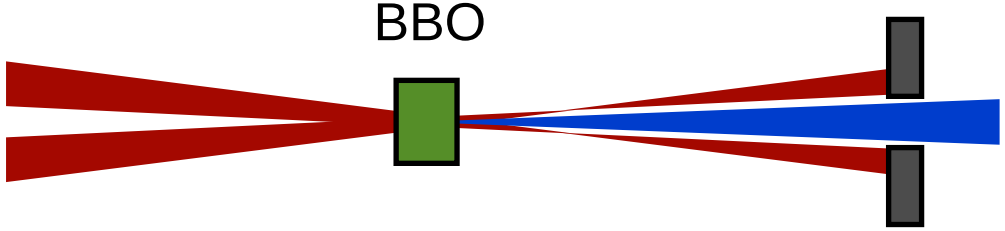

Raoult et al. *Opt. Lett.* **1998**, *23*, 1117

Positive
Chirp

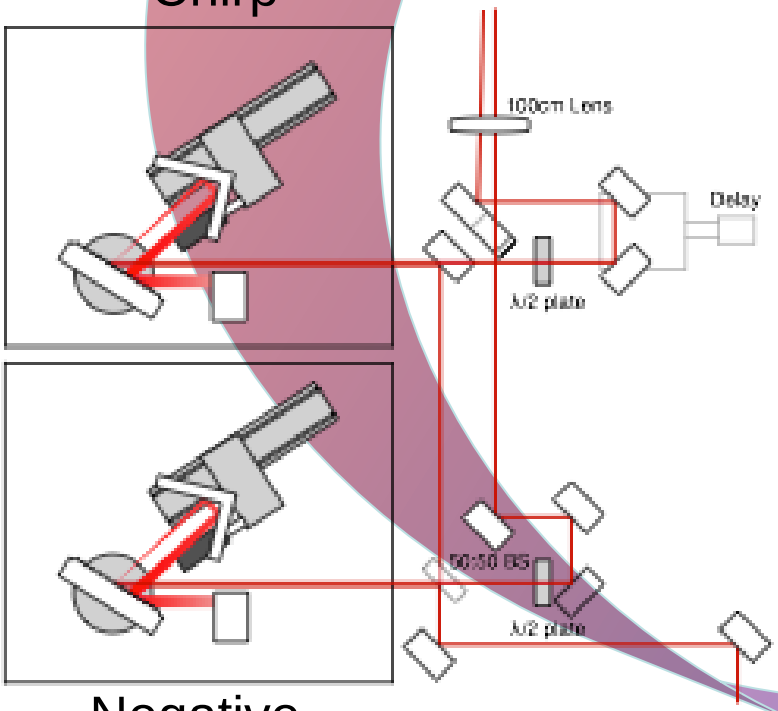

Negative
Chirp

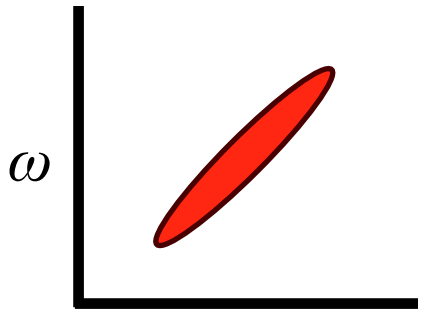

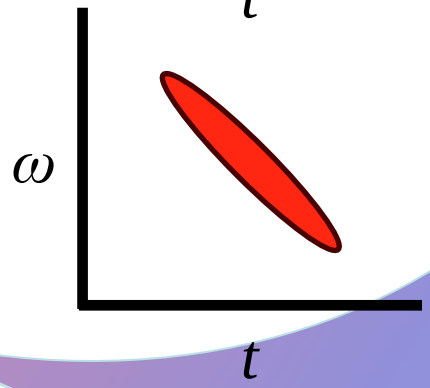

Narrow-band
400 nm
2 ps
7 cm^{-1}

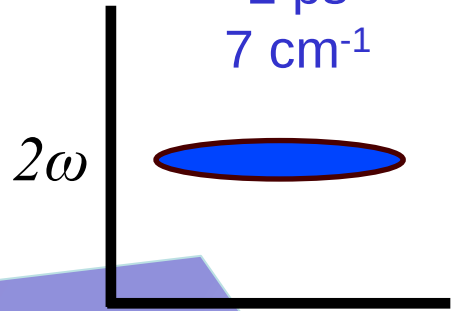

Electronic SHG spectrometer (500-950 nm)

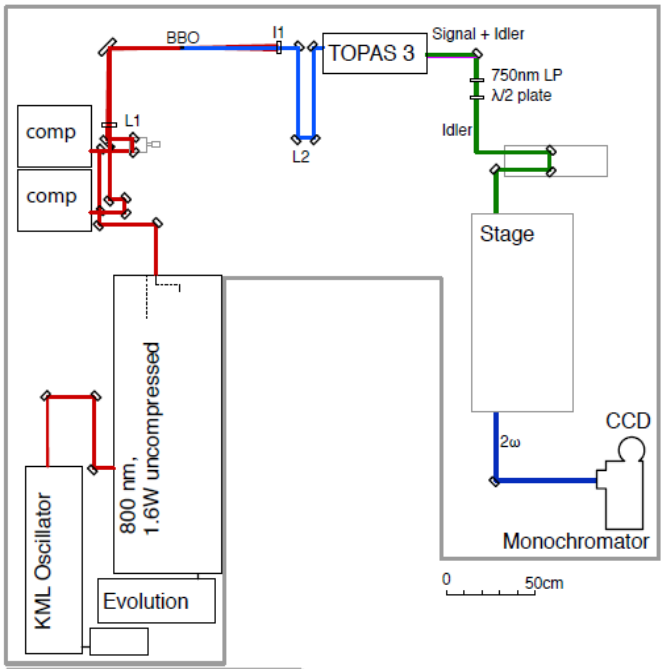

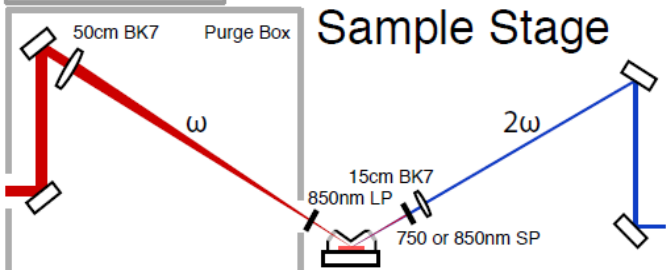

eSHG

surface-selective

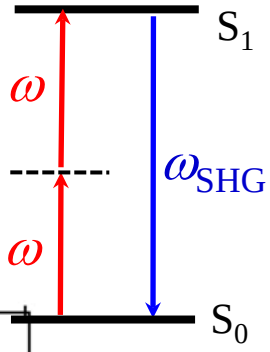

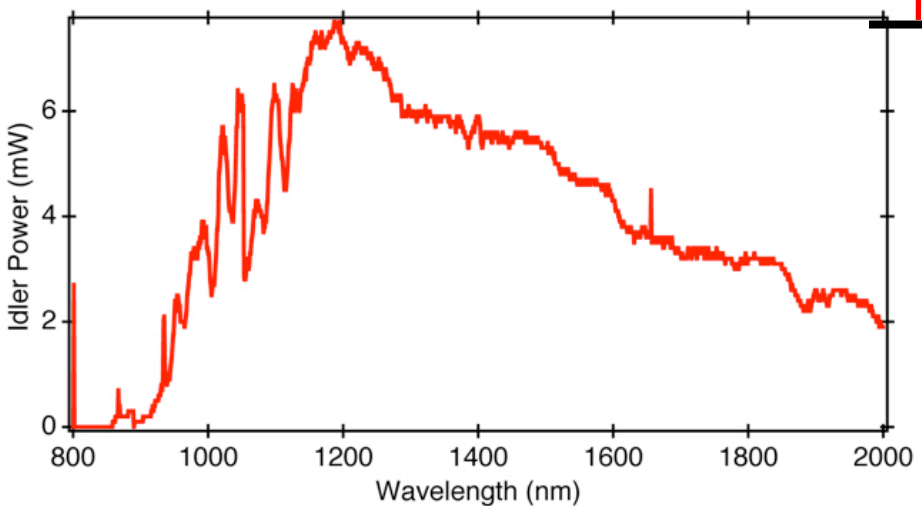

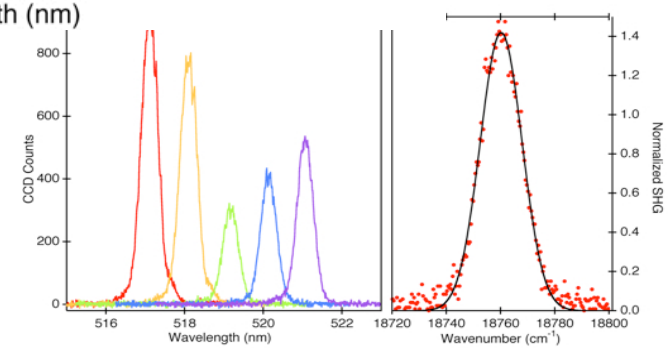

Samples

UV-Vis

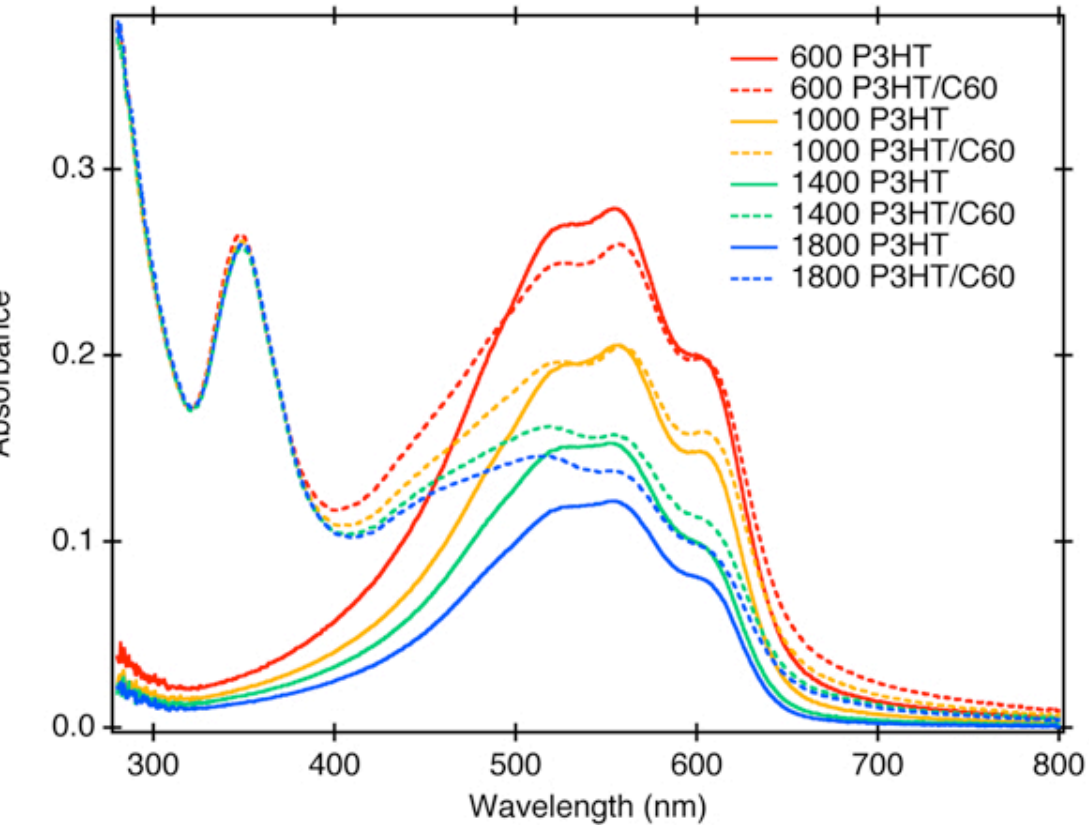

AFM

Spin-cast @ 600 rpm

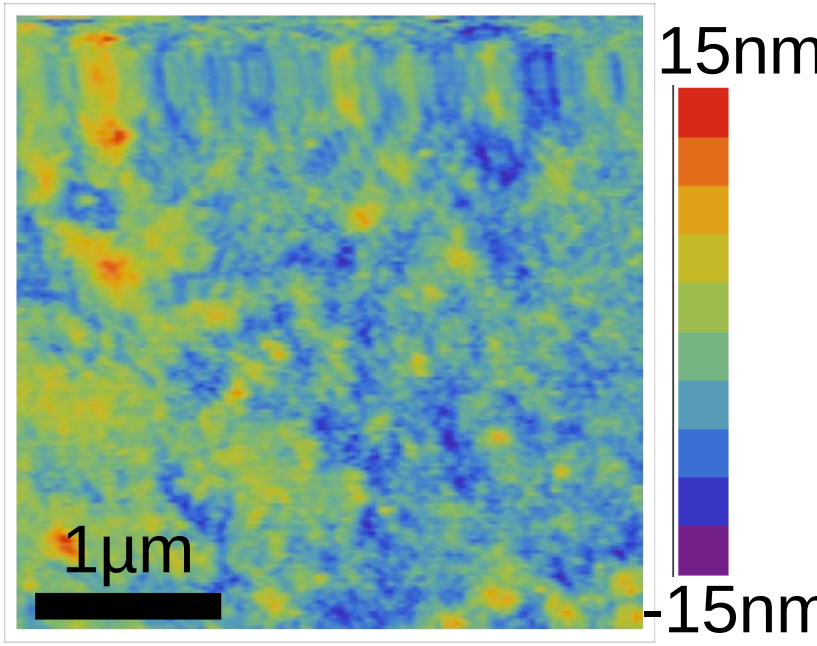

RMS Roughness 3.9nm

4 P3HT samples:
Thickness 38nm, 27nm, 20nm, 16nm

4 samples P3HT/15 nm C_{60}

SHG Spectra of P3HT and P3HT/C_{60} films
Raw data

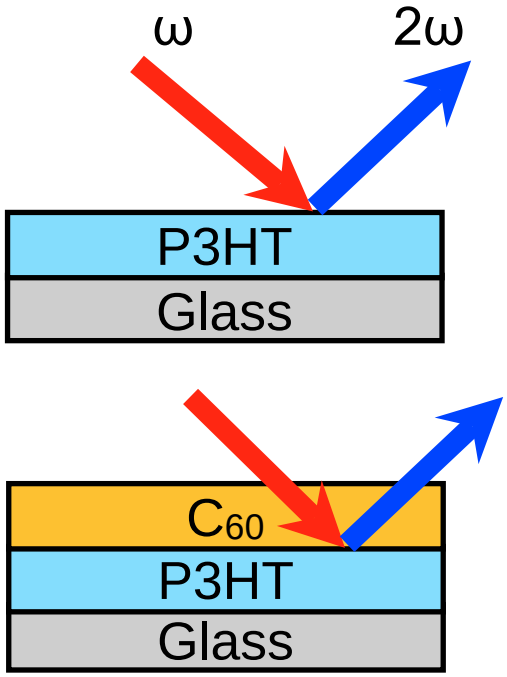

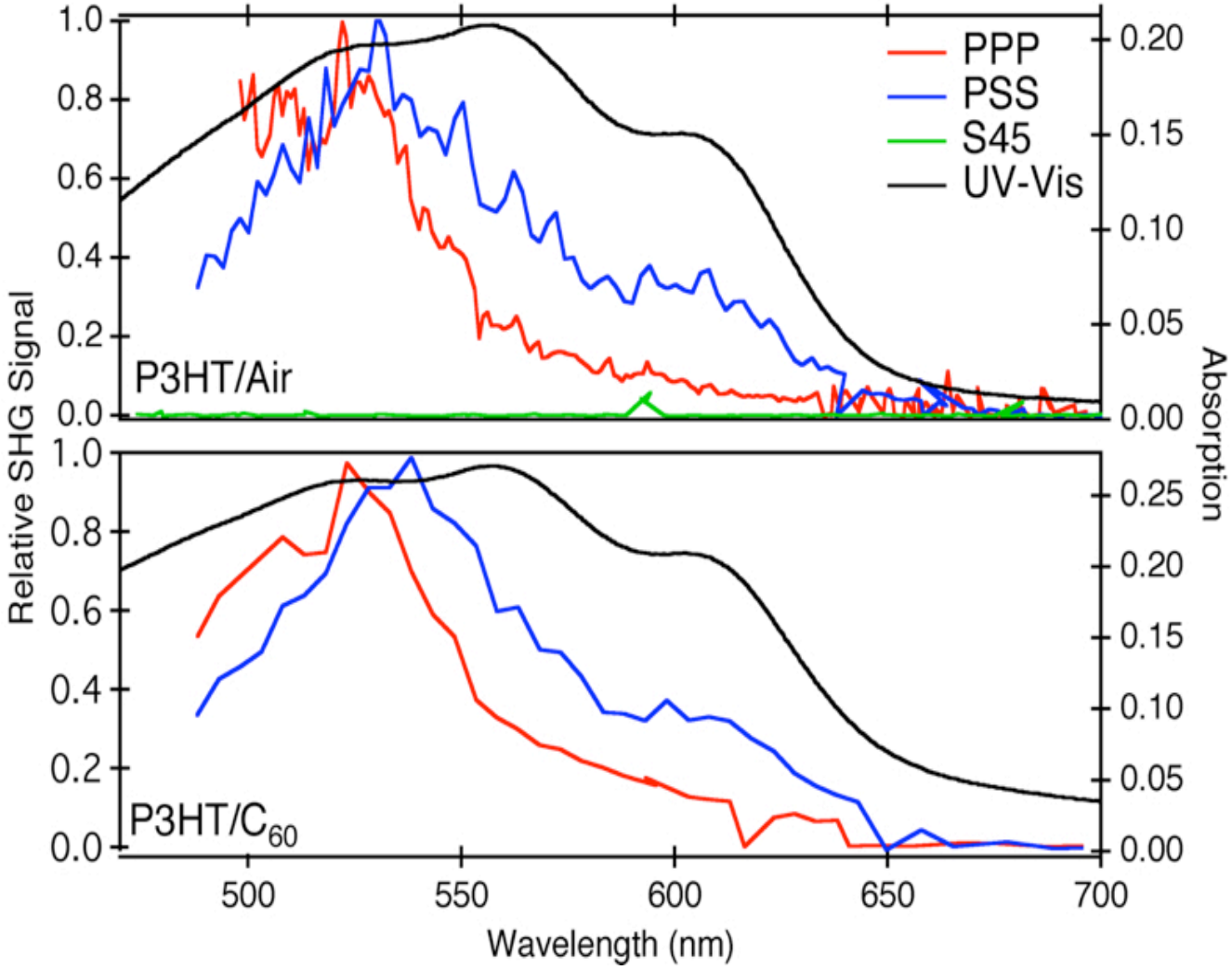

Model for thickness dependence

$$I_{SHG}(\omega) \propto \frac{\omega^2}{n(2\omega)n(\omega)^2}\left|\chi^{(2)}_{Surface} + e^{i\theta}\chi_{Bulk}(\omega)Thickness\right|^2 I(\omega)^2$$

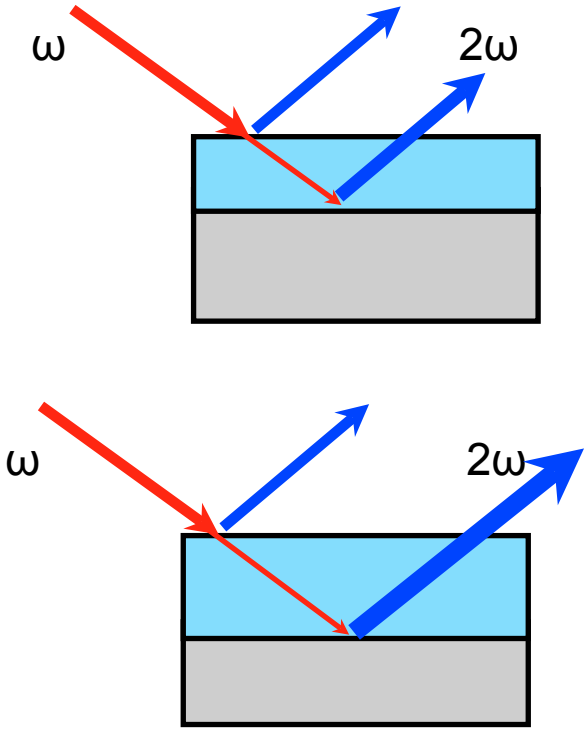

SHG (PSS) signal at 490nm

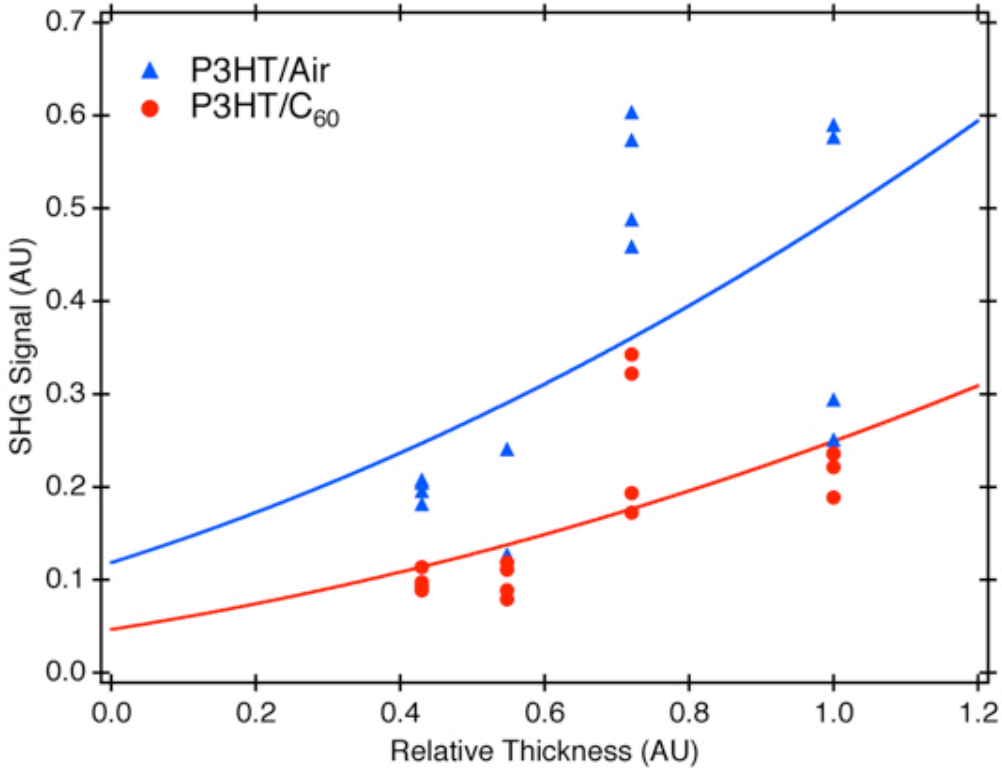

Separation of surface vs bulk SHG signal for P3HT and P3HT /C_{60}

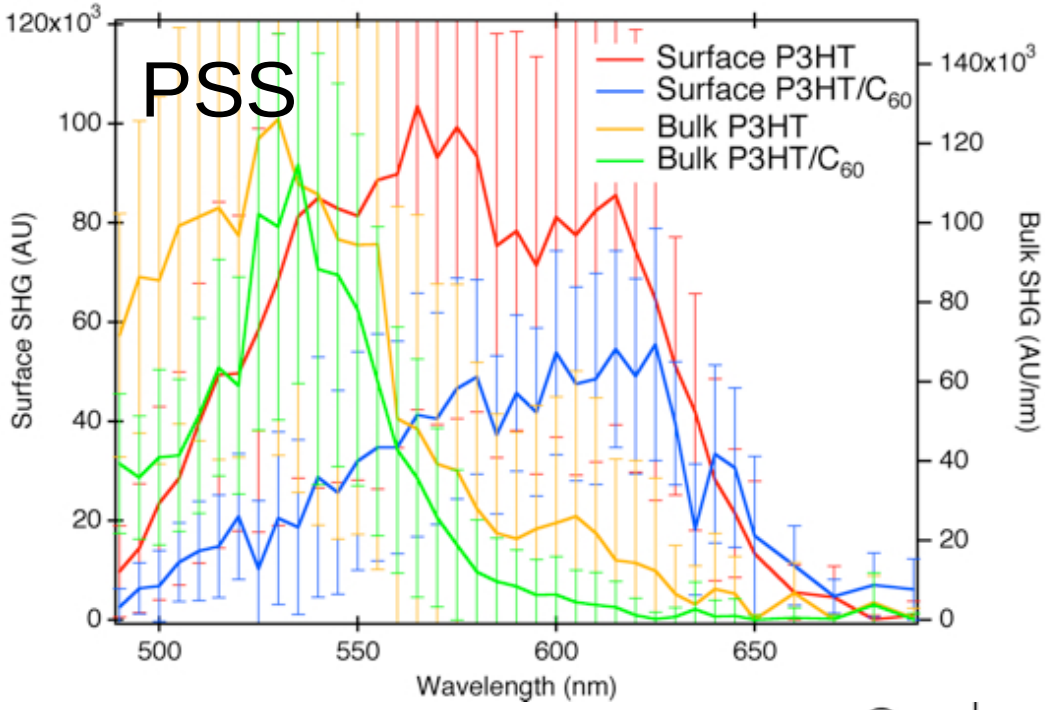

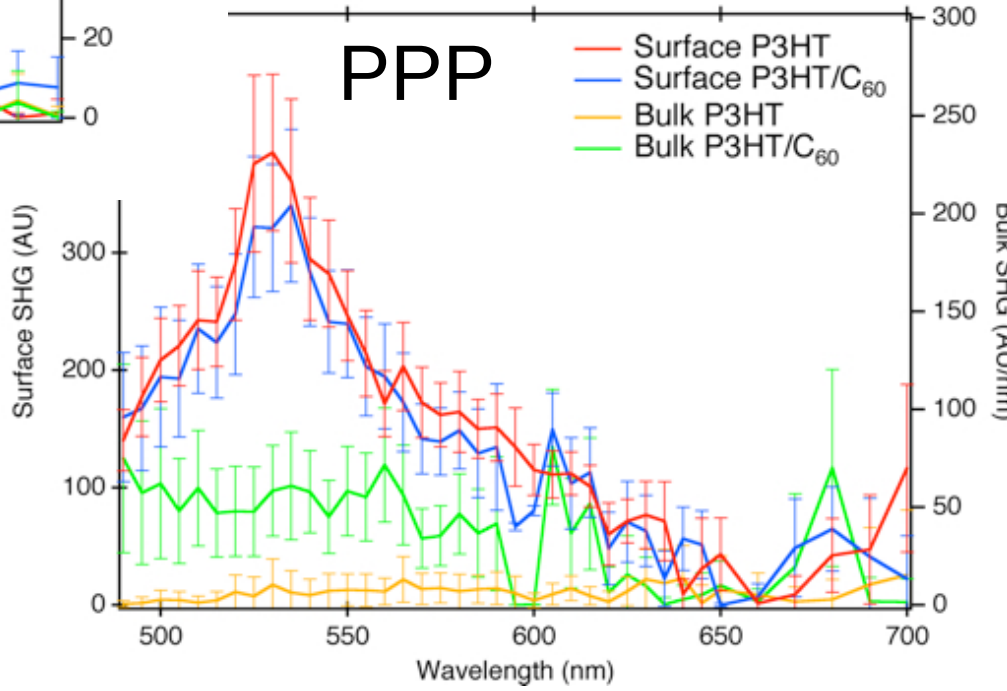

A Model for the Signal

PSS

$$\chi^{(2)}_{eff,PSS} = \chi_{yyz}\, L_{zz}(2\omega)\, L_{yy}(\omega)\, L_{yy}(\omega)\, \sin(\beta)$$

PPP

$$\chi^{(2)}_{eff,PPP} = -\chi_{xxz}\, L_{zz}(2\omega)\, L_{xx}(\omega)\, L_{xx}(\omega)\, \cos(\beta)^2 \sin(\beta)$$
$$-\chi_{xzx}\, L_{xx}(2\omega)\, L_{xx}(\omega)\, L_{zz}(\omega)\, \cos(\beta)^2 \sin(\beta)$$
$$+\chi_{zxx}\, L_{xx}(2\omega)\, L_{zz}(\omega)\, L_{xx}(\omega)\, \cos(\beta)^2 \sin(\beta)$$
$$+\chi_{zzz}\, L_{zz}(2\omega)\, L_{zz}(\omega)\, L_{zz}(\omega)\, \sin(\beta)^3$$

Electronic properties of molecules

Frequency-dependent Fresnel factors

Experimental geometry

Optical Data for P3HT/air and P3HT/C_{60} Interface

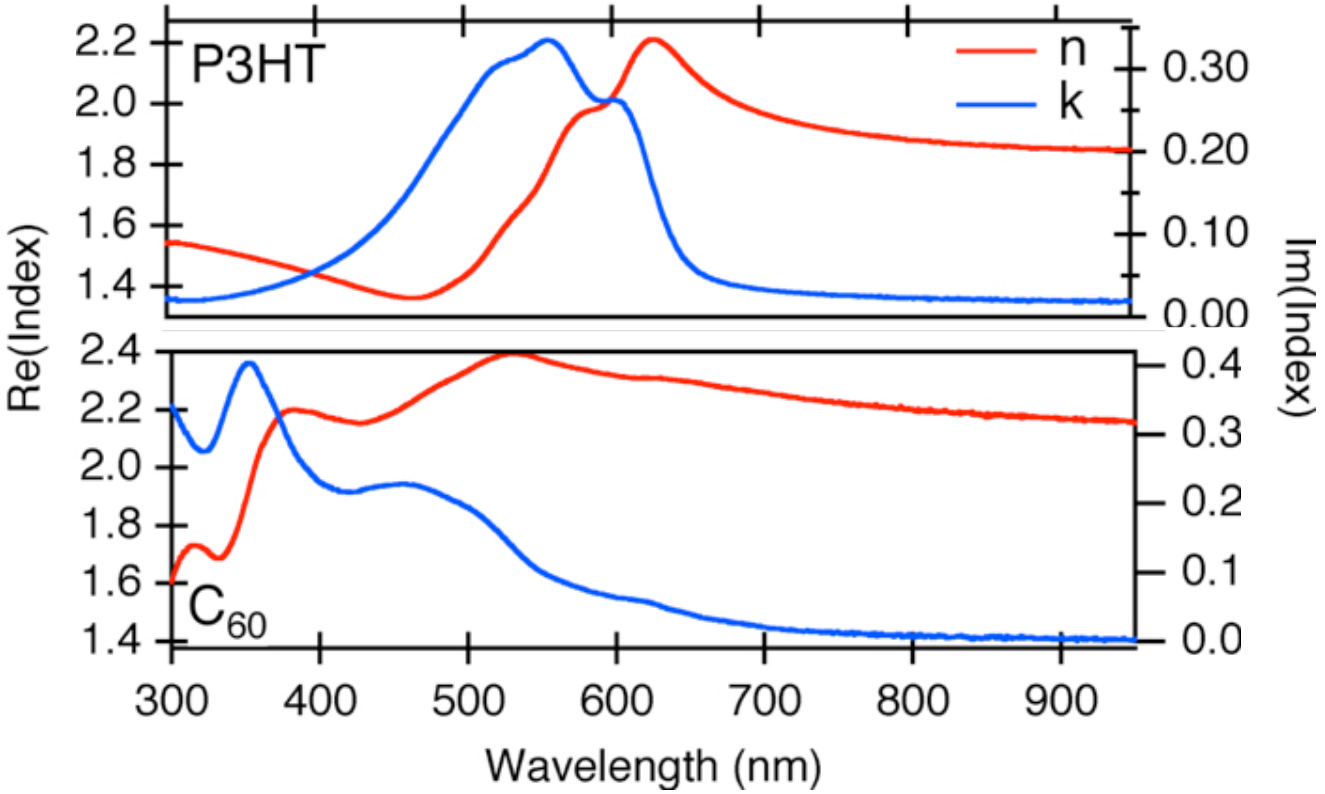

Re(Index) constant through IR

Im(Index) = 0 through IR

Electronic structure at D/A interfaces by SHG spectroscopy

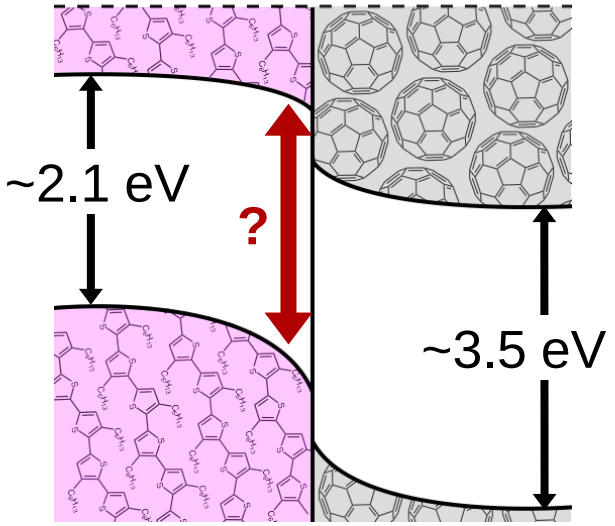

PSS

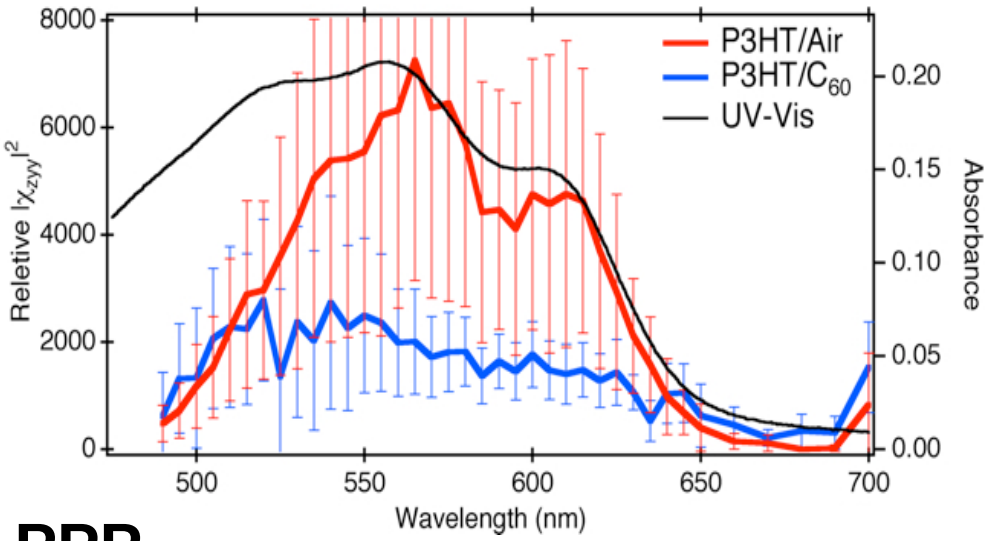

PPP

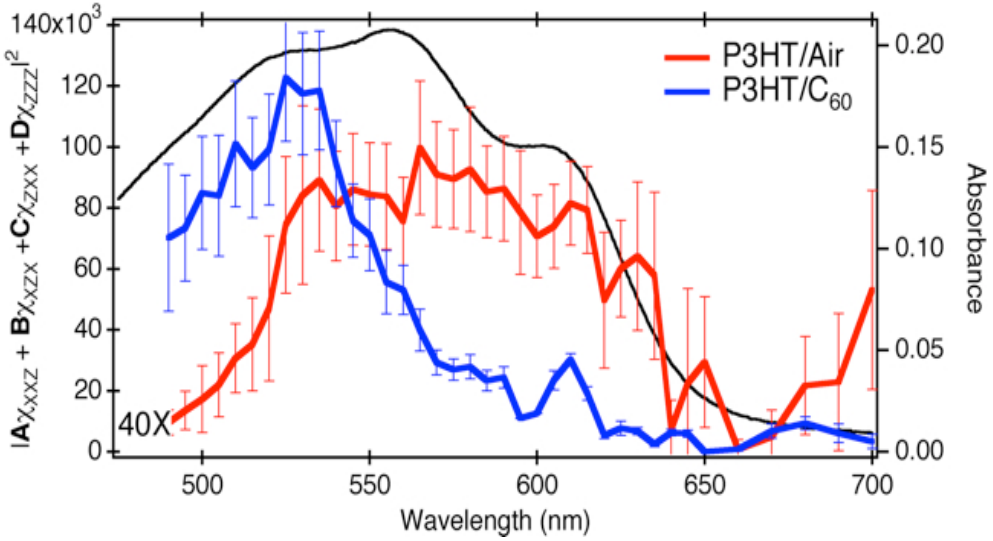

- P3HT/air interface: same spectrum as bulk P3HT (no band bending)
- Blue shift/new states (?) at P3HT/C60 interface

1-photon vs. 2-photon absorption of hexithiophene

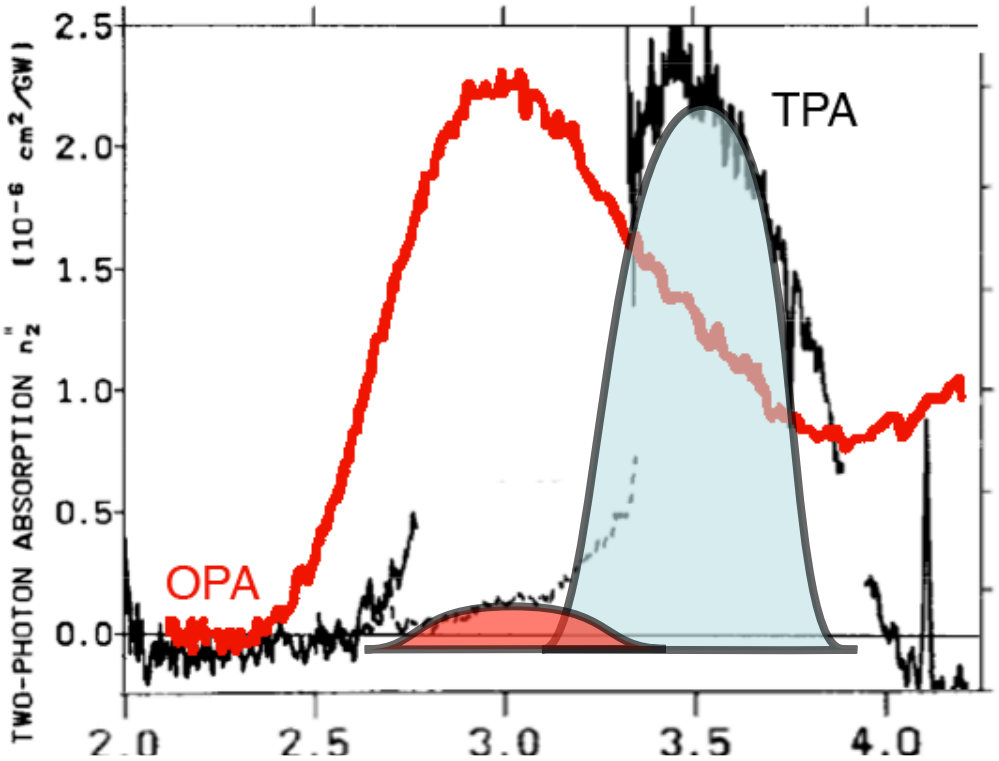

$^1B_u \leftarrow {}^1A_g$ $^2A_g \leftarrow {}^1A_g$

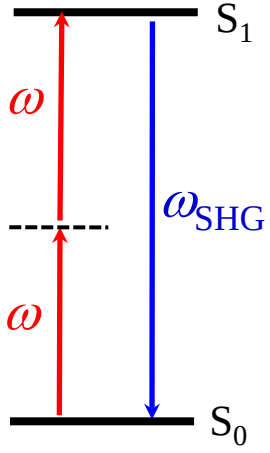

2-PA:
only $^2A_g \leftarrow {}^1A_g$ allowed

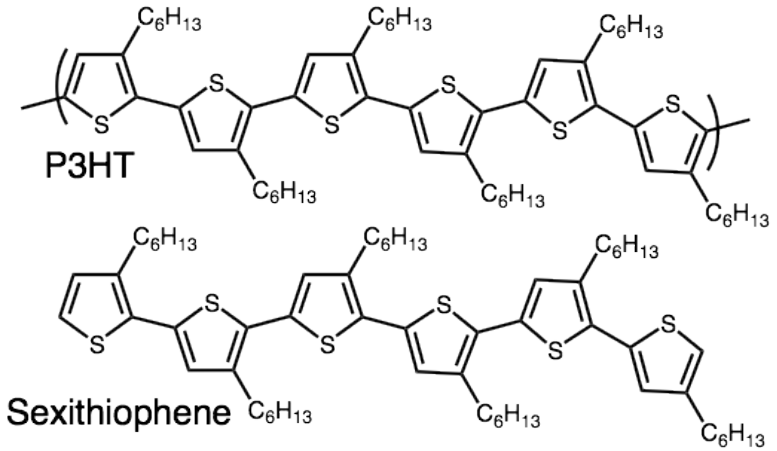

SHG:
both modes may be allowed

eSHG spectroscopy of red-absorbing polymers

(Barry Thompson's group)

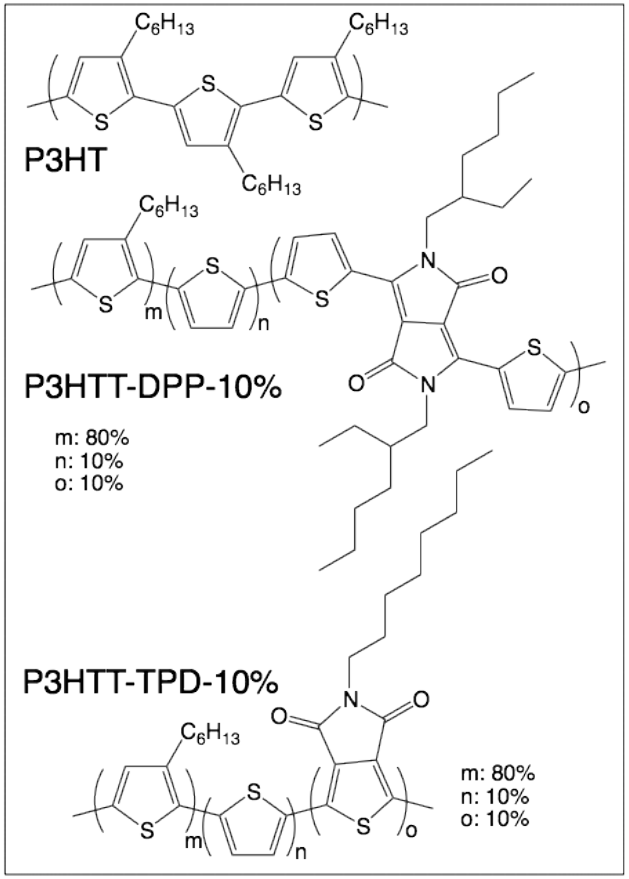

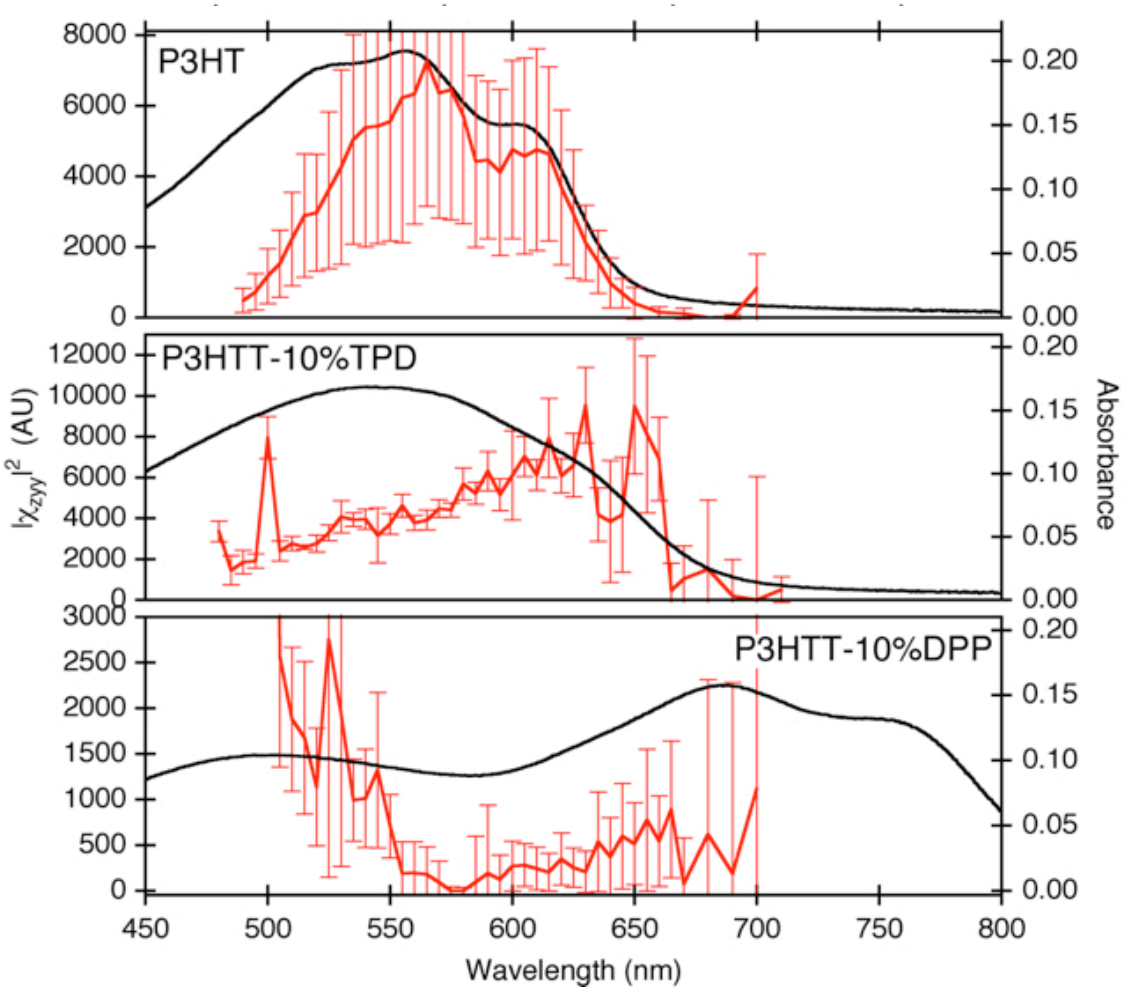

Acknowledgments

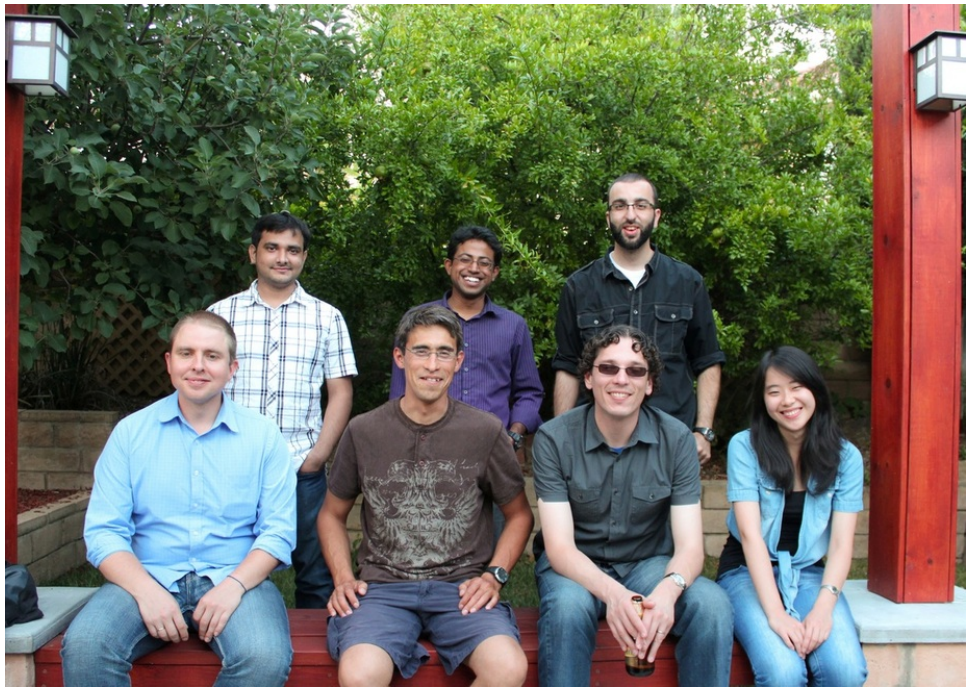

Postdocs:
Sergey Malyk
Sean Roberts

Grad. students:
Purnim Dhar
David Valley
Fadel Shalhout
Chayan Dutta
Dritiman Bhatchatarya
Angelo Montenegro
Mikhail Vinaykin

OPV materials:
Prof. Barry Thompson & group (USC)
Prof. Mark Thompson & group (USC)

Funding:
CEN CENTER FOR ENERGY NANOSCIENCE DOE
NSF
US AFOSR
USC

Surface Selective Nonlinear (Even-order) Optical Spectroscopies

Polarization in medium

$$\vec{P}(t) = \vec{P}^{(0)} + \vec{P}^{(1)} + \boxed{\vec{P}^{(2)}} + \vec{P}^{(3)} + \ldots$$

$$= \vec{P}^{(0)} + \chi^{(1)}\vec{E} + \boxed{\chi^{(2)} : \vec{E}\vec{E}} + \chi^{(3)} : \vec{E}\vec{E}\vec{E} + \ldots$$

Apply inversion operation to $P^{(2)}$:

$$\vec{P}^{(2)} = \chi^{(2)} : \vec{E}_\omega \vec{E}_\omega$$

$$\hat{i}\,\chi^{(2)} = \chi^{(2)} \quad \textbf{in isotropic media}$$

$$\hat{i}\vec{P}^{(2)} = \hat{i}\left(\chi^{(2)} : \vec{E}_\omega \vec{E}_\omega\right)$$

$$-\vec{P}^{(2)} = \chi^{(2)} : \left(-\vec{E}_\omega\right)\left(-\vec{E}_\omega\right) = \vec{P}^{(2)}$$

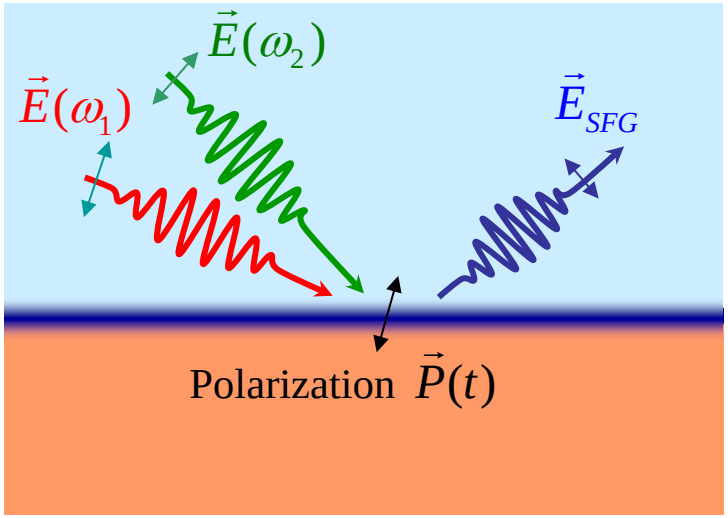

Surface selectivity: $\chi^{(2n)} \neq 0$ only at interface

P3HT/C_{60} Interface SHG

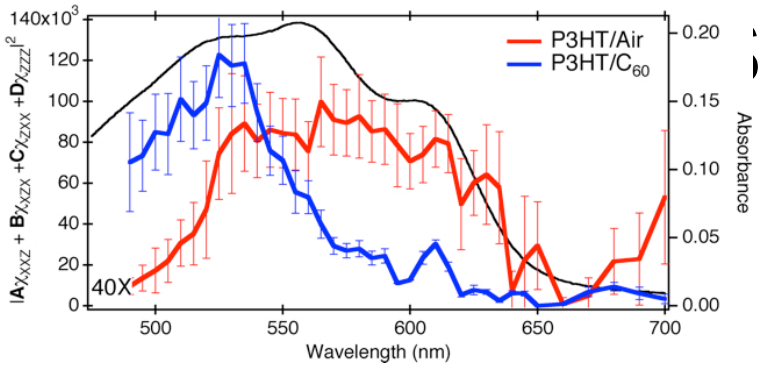

Observe a blue shift from P3HT/air interface to P3HT/C_{60} interface

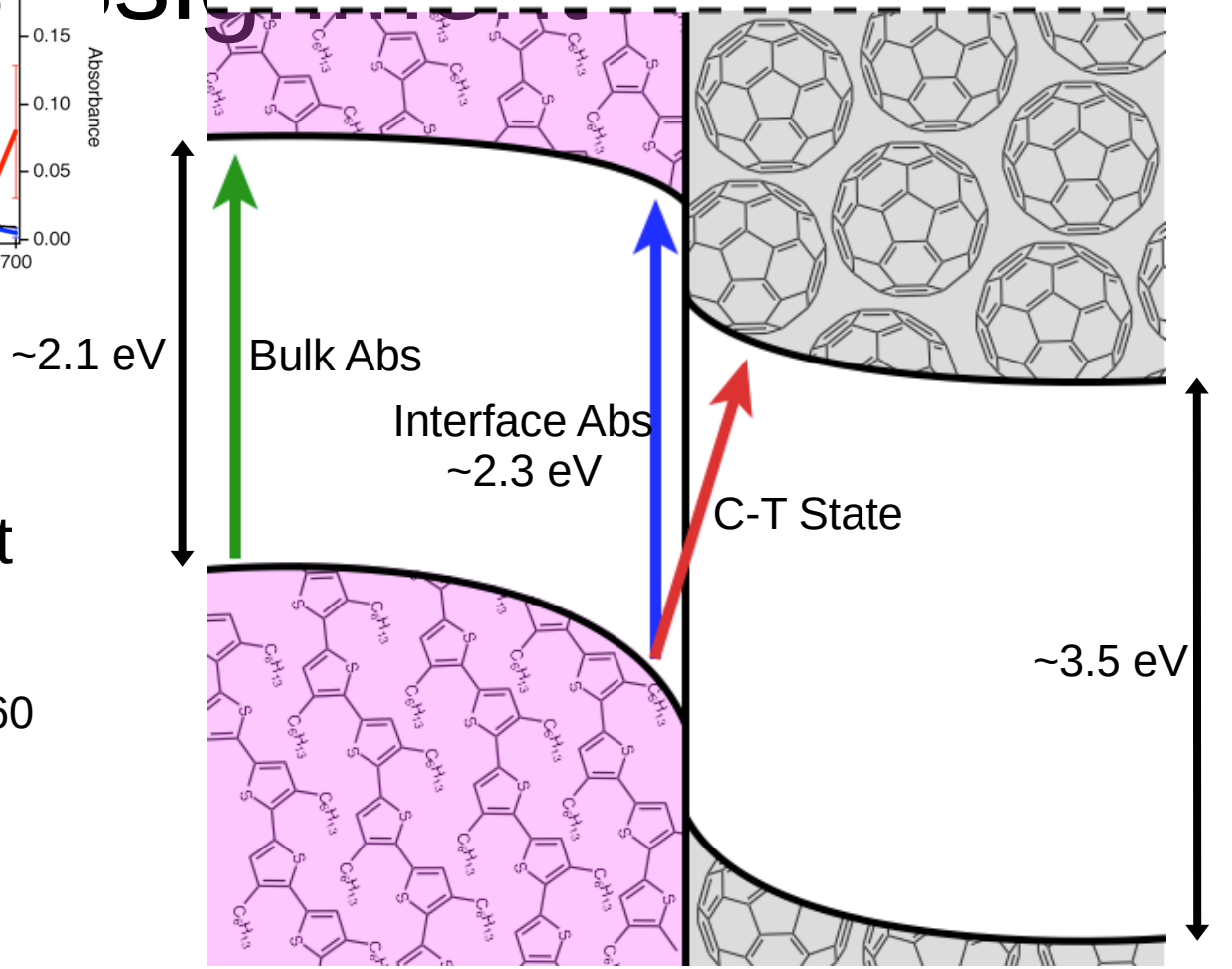

Methylated Si(111)

Nate Lewis and coworkers, *Caltech*

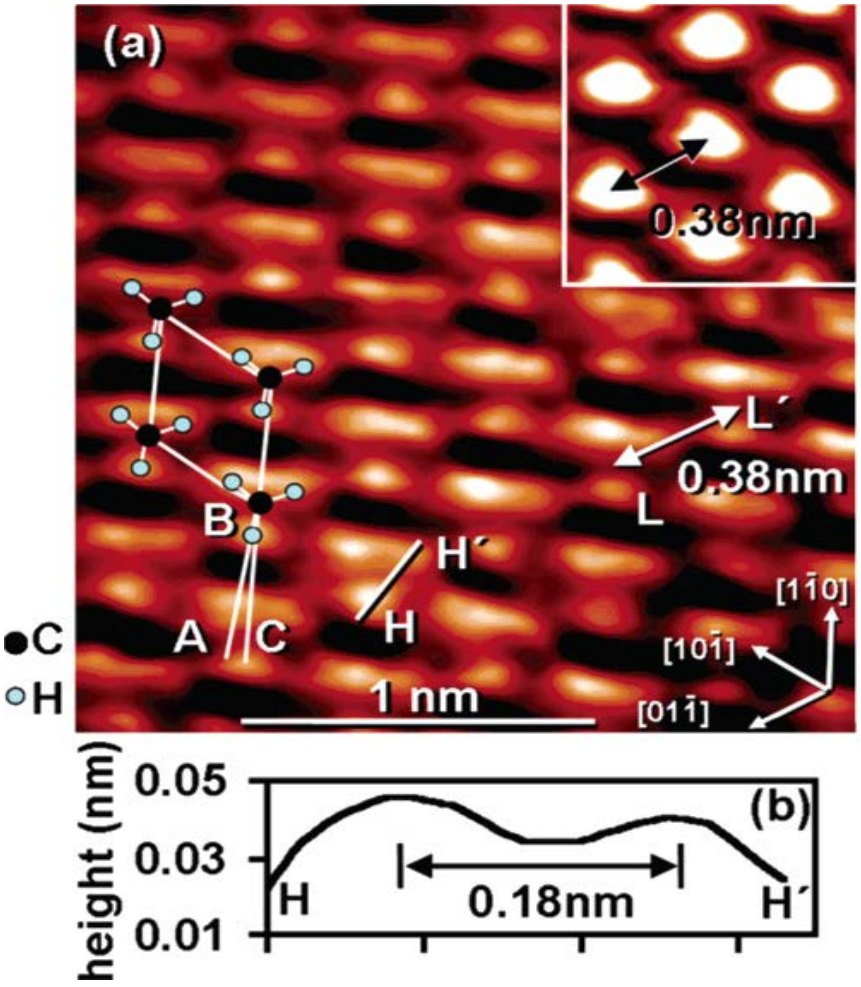

Hongbin Yu *et al. Phys. Chem. B,* **109** (2005)

STM Studies

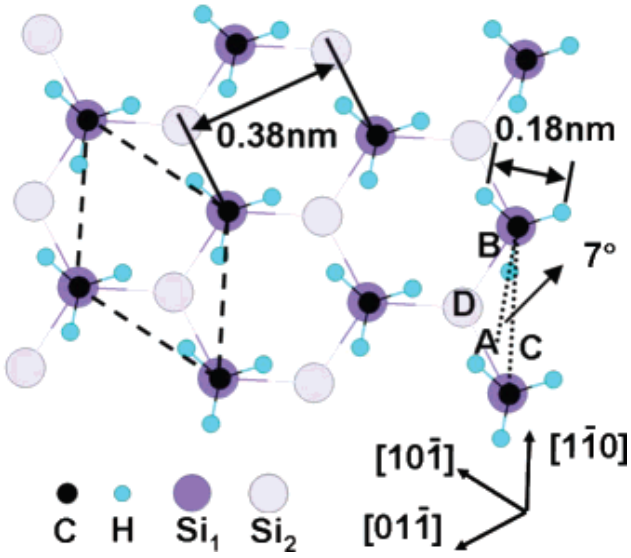

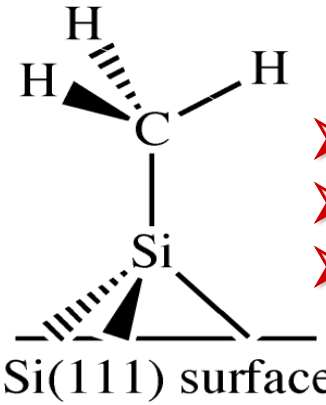

- Surface coverage?
- Orientation?
- Rotational motion?

VSFG spectra of Methylated Si(111)

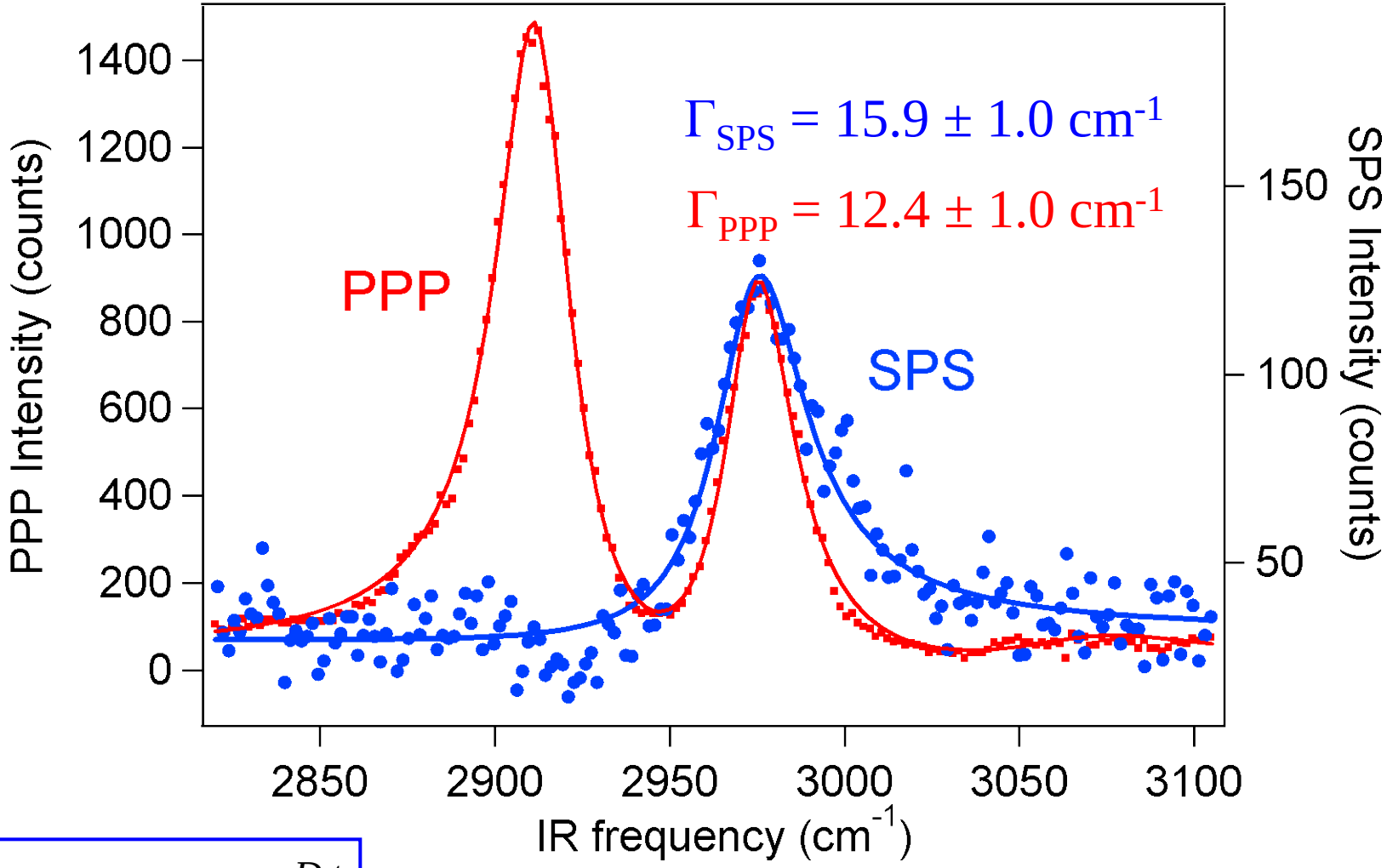

$$\chi^{(2)}_{SPS}(t) \propto e^{-D_{\parallel} t}$$

Γ_{rot} = 3.5 ± 1.5 cm^{-1} **τ_{rot} = 1-2 ps**

Malyk, Shalhout, O'Leary , Lewis, Benderskii *JPC C* 117, 935 (2013)

Rotation of methyl groups

4 K

Frozen on STM time scale

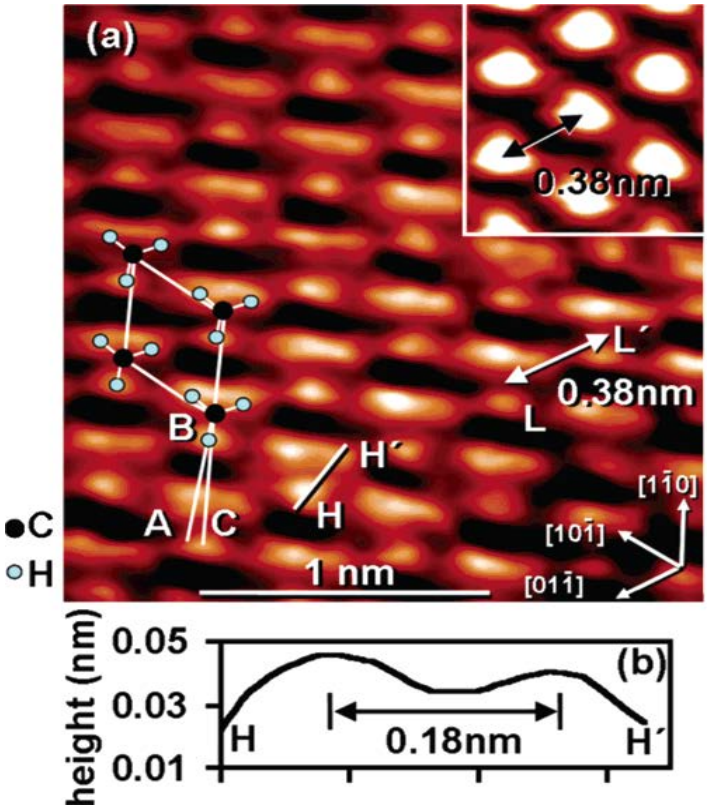

Room T

Experimental rotational dephasing:

$\Gamma_{rot} = \Gamma_{SPS} - \Gamma_{PPP} \approx$ **3.5 cm^{-1}** → $\tau_{rot} \sim$ **1.5 ps**

Free methyl rotational dephasing at room T:

$\tau_{rot} \sim$ **100 fs**

(classical free-rotor correlation function)

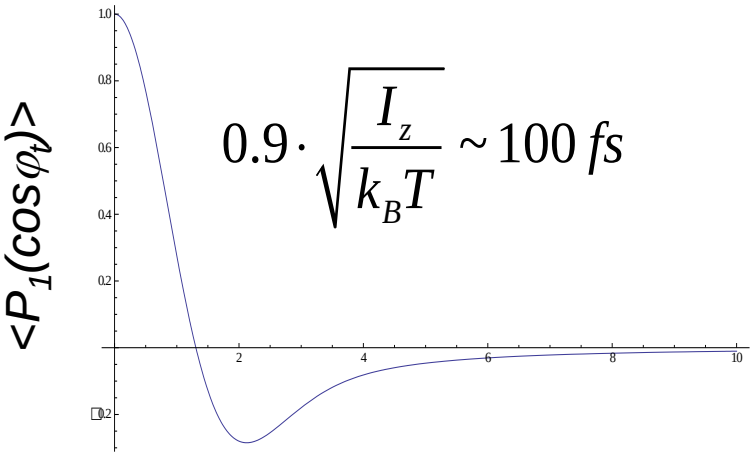

$$0.9 \cdot \sqrt{\frac{I_z}{k_B T}} \sim 100\ fs$$

Classical free-rotor correlation function

$$C(t) = \langle \mu(0) \cdot \mu(t) \rangle = \langle P_1(\cos\theta_t) \rangle = \frac{I_z}{k_B T} \int_0^{\infty} \cos(\Omega t) \cdot \Omega \cdot \exp\left(-\frac{I_z \Omega^2}{2 k_B T} \right) d\Omega$$

SFG of dodecanethiol SAM on flat gold

SFG spectrum
Polarization *PPP* (SFG-vis-IR)

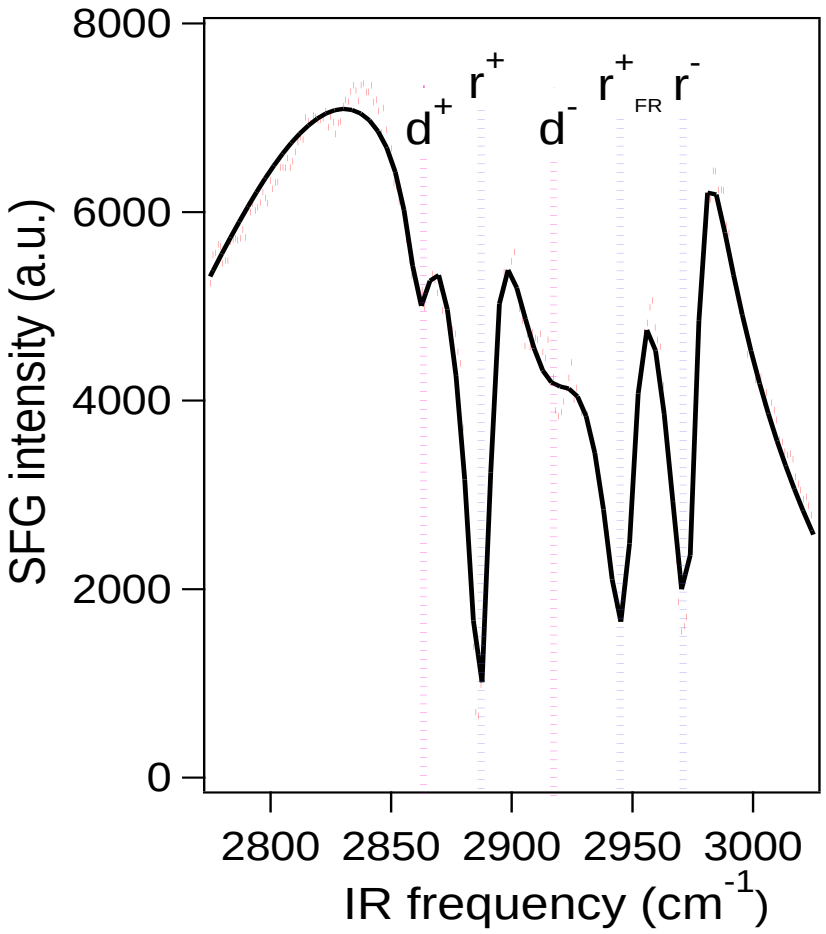

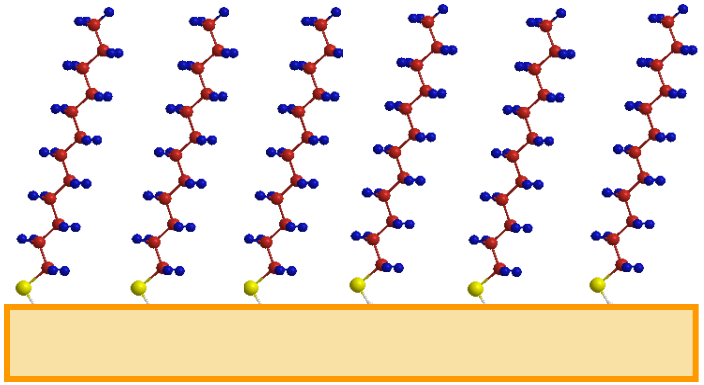

Nearly all-*trans* conformation (SFG propensity rule)

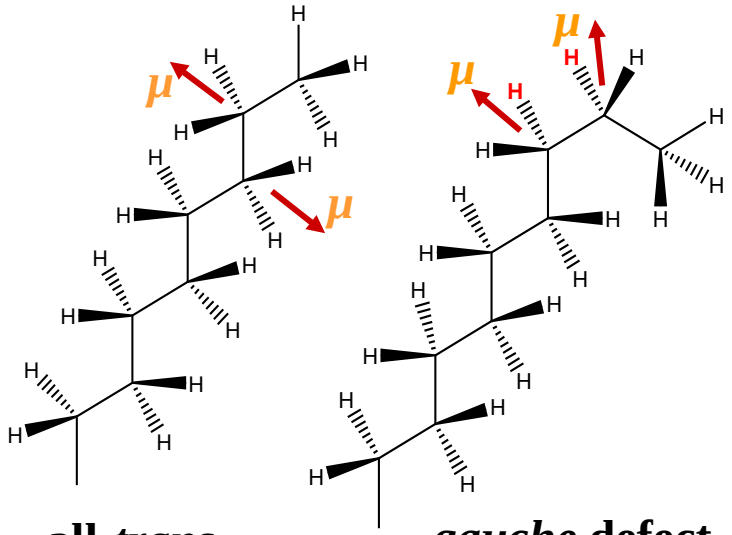

all-*trans* ***gauche*** **defect**

TEM 1-dodecanethiol capped Au NPs

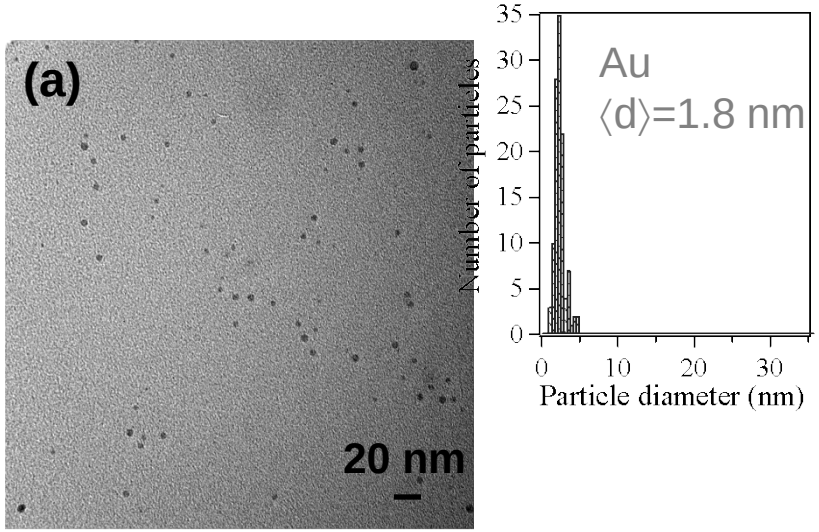

51.8 nm^2/particle (5% monolayer)

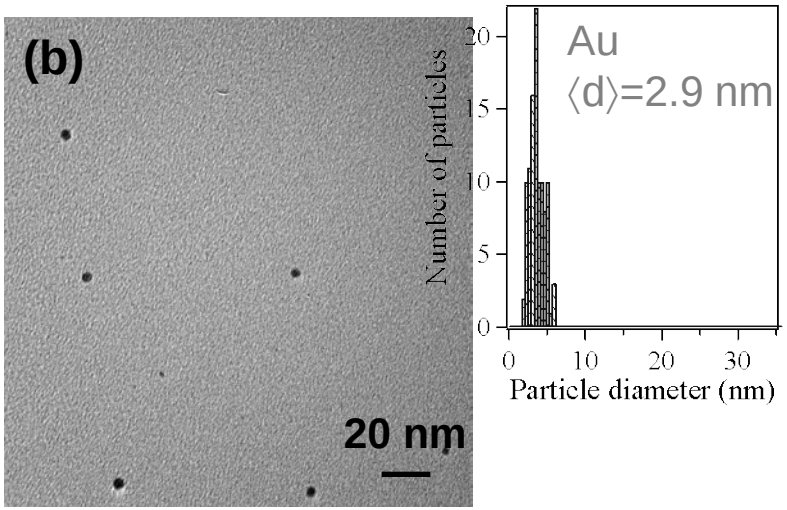

(51.8 nm^2/particle (14% monolayer)

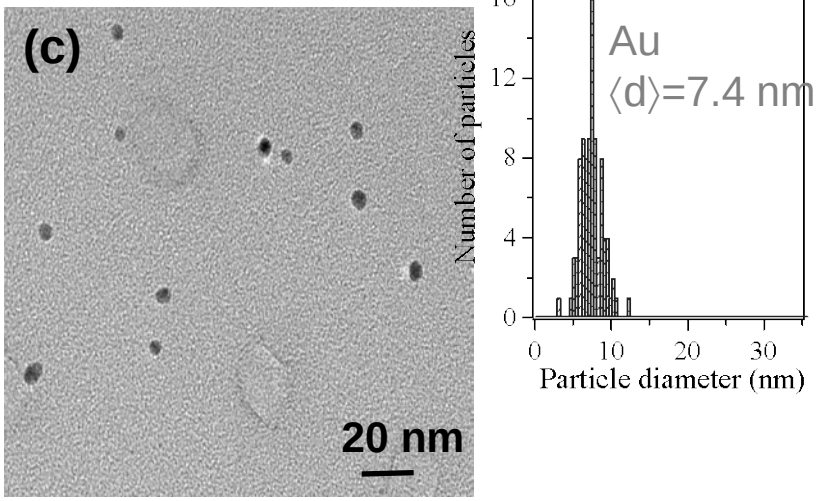

712 nm^2/particle (7% monolayer)

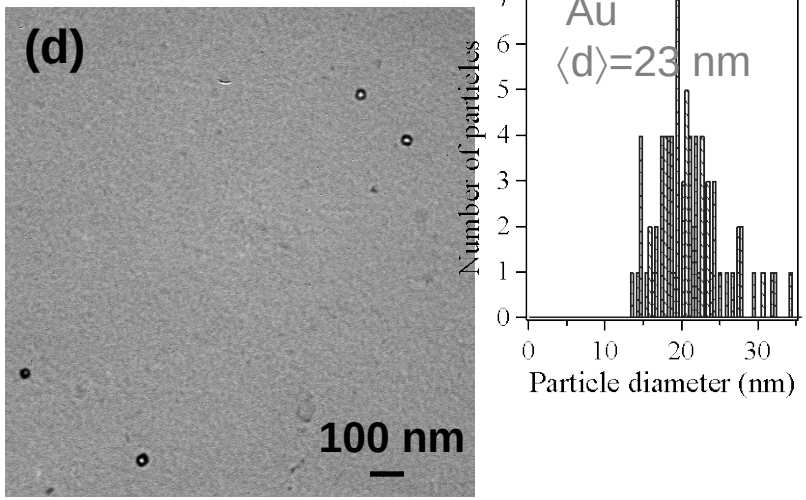

14200 nm^2/particle (3% monolayer)

SFG of dodecanethiol on gold nanoparticles

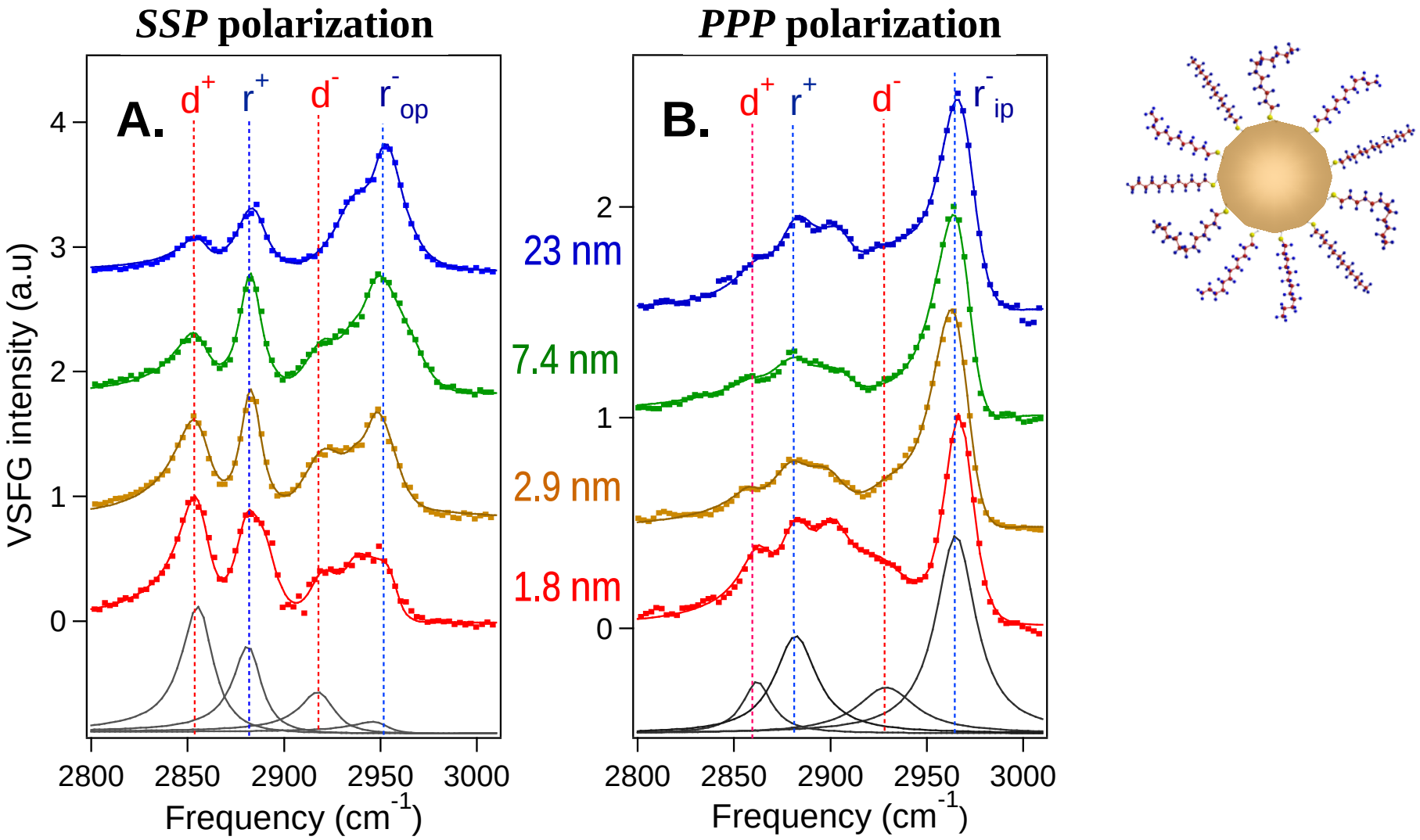

C. Weeraman, A.Yatawara, A.N.Bordenyuk, A.V.Benderskii *JACS* **128**, 14244 (2006)
A.N. Bordenyuk *et al.* *JPC C* 111, 8925 (2007)

Size-dependent d/r ratio in SFG spectra

Dodecanethiol on gold NP

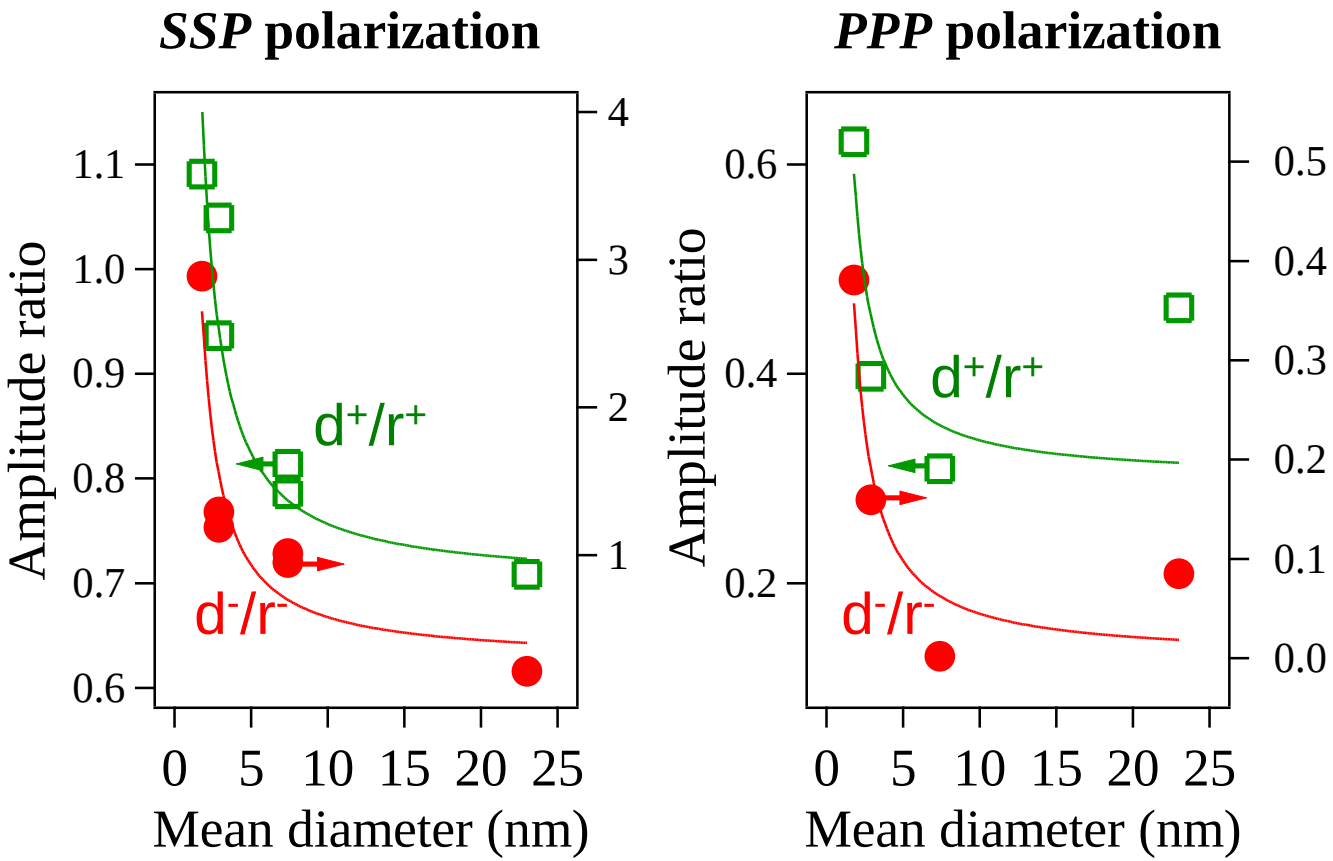

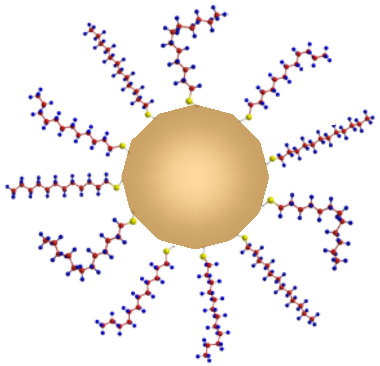

C. Weeraman, A.Yatawara, A.N.Bordenyuk, A.V.Benderskii *JACS* **128**, 14244 (2006)
A.N. Bordenyuk *et al.* *JPC C* 111, 8925 (2007)

Size-dependent *gauche* defects

***Cylindrical volume* (flat surface)** $V_0 = aL$

***Conical volume* (curved surface)** $V = \frac{\Phi}{3}\left[(R+L)^3 - R^3\right]$

Solid angle $\Phi = a / R^2$

Φ = solid angle

L = chain length

R = particle radius

a = area per head group

Fractional additional volume for *gauche* defects

$$\delta(R) \propto \frac{V - V_0}{V_0} = x + \frac{1}{3}x^2$$

$x = L / R$

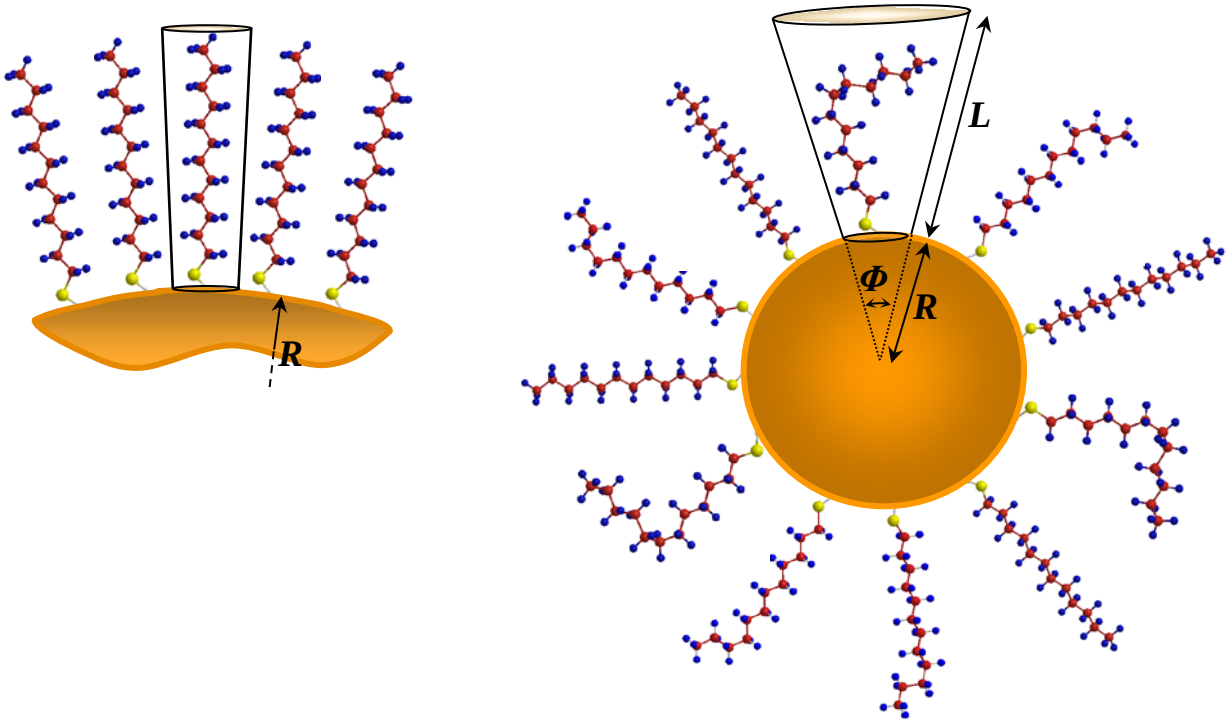

TEM 1-dodecanethiol capped Ag NPs

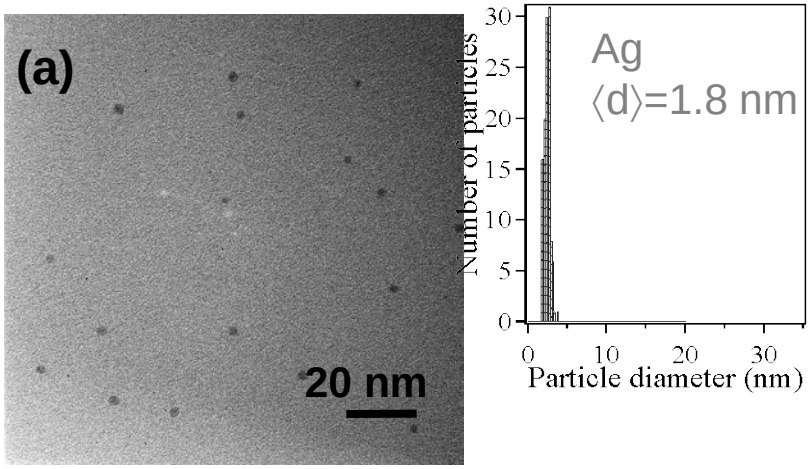

25.2 nm^2/particle (11% monolayer)

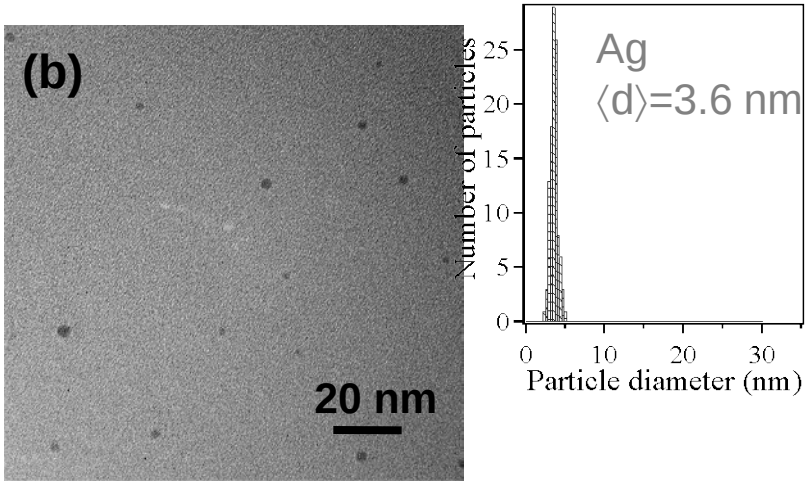

201 nm^2/particle (5% monolayer)

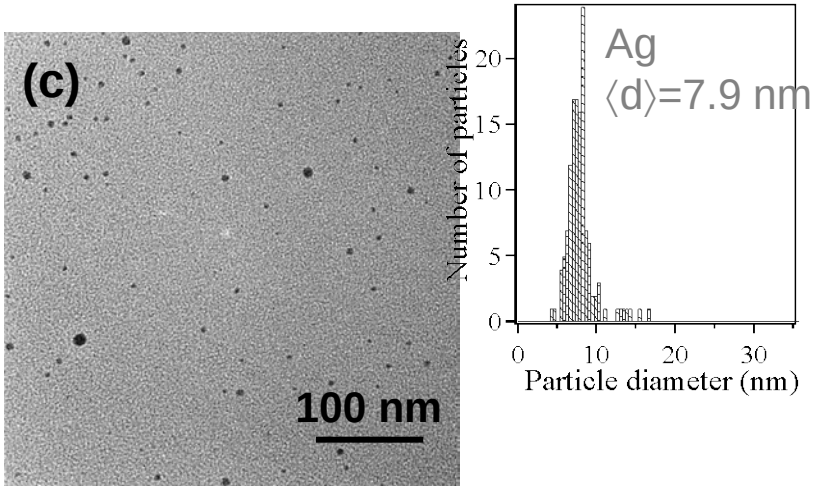

2130 nm^2/particle (1% monolayer)

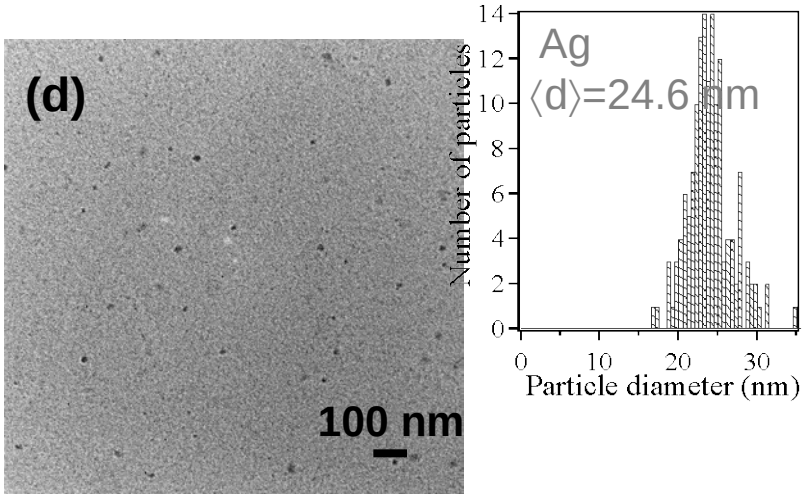

64300 nm^2/particle (1% monolayer)

SFG of dodecanethiol on silver nanoparticles

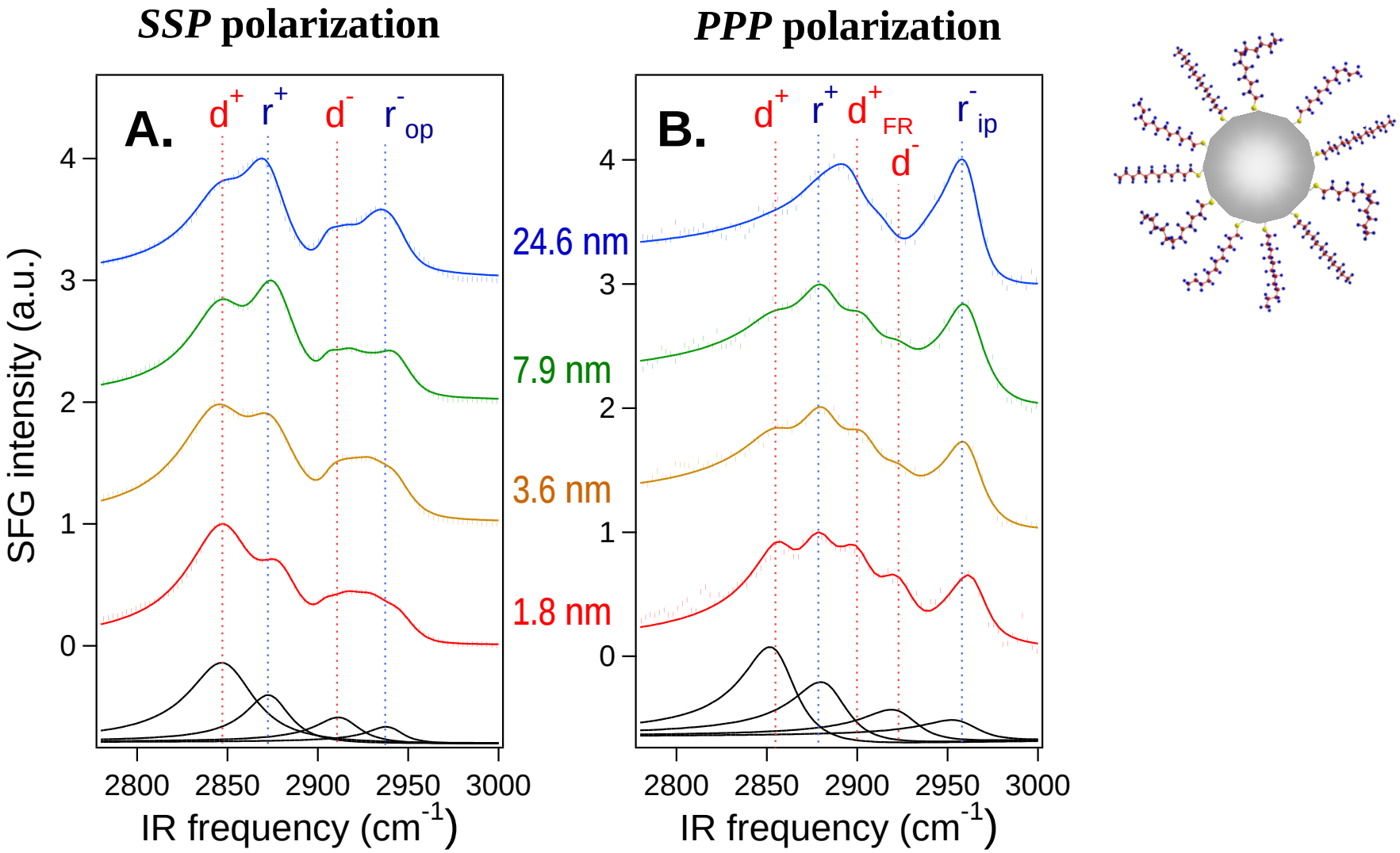

A.N. Bordenyuk *et al.* *JPC C* 111, 8925 (2007)

$$X^{(2)}_{eff,IJK} = \sum_{ijk} L_{ii}(\omega_{SFG}) L_{jj}(\omega_{vis}) L_{kk}(\omega_{IR}) \left(\hat{i}\cdot\hat{I}_{SFG}\right)\left(\hat{j}\cdot\hat{J}_{vis}\right)\left(\hat{k}\cdot\hat{K}_{IR}\right)\chi^{(2)}_{ijk}$$

$\chi^{(2)}_{ijk}$ - macroscopic surface susceptibility tensor,
i, j, k - unit vectors along the lab axes x, y, z and
I_{SFG}, J_{vis}, K_{IR} - unit vectors along the polarization of the fields
$L_{ii}(\square)$ (i = x, y, z) represent local field corrections at the surface for a frequency $\square$

$$X^{(2)}_{eff,SSP} = L_{yy}(\omega_{SFG}) L_{yy}(\omega_{vis}) L_{zz}(\omega_{IR}) \sin\alpha_2 \chi^{(2)}_{yyz}$$

$$X^{(2)}_{eff,SPS} = L_{yy}(\omega_{SFG}) L_{zz}(\omega_{vis}) L_{yy}(\omega_{IR}) \sin\alpha_1 \chi^{(2)}_{yzy}$$

$$\begin{aligned} X^{(2)}_{eff,PPP} = & -L_{xx}(\omega_{SFG}) L_{xx}(\omega_{vis}) L_{zz}(\omega_{IR}) \cos\alpha \cos\alpha_1 \sin\alpha_2 \chi^{(2)}_{xxz} \\ & -L_{xx}(\omega_{SFG}) L_{zz}(\omega_{vis}) L_{xx}(\omega_{IR}) \cos\alpha \sin\alpha_1 \cos\alpha_2 \chi^{(2)}_{xzx} \\ & +L_{zz}(\omega_{SFG}) L_{xx}(\omega_{vis}) L_{xx}(\omega_{IR}) \sin\alpha \cos\alpha_1 \cos\alpha_2 \chi^{(2)}_{zxx} \\ & +L_{zz}(\omega_{SFG}) L_{zz}(\omega_{vis}) L_{zz}(\omega_{IR}) \sin\alpha \sin\alpha_1 \sin\alpha_2 \chi^{(2)}_{zzz} \end{aligned}$$

$\chi^{(2)}_{xxz} = \chi^{(2)}_{yyz}$ $\chi^{(2)}_{zyy} = \chi^{(2)}_{zxx}$ $\chi^{(2)}_{xzx} = \chi^{(2)}_{yzy}$ $\chi^{(2)}_{zzz}$ only 7 none-zero components (4 independent)

$$\chi_{ijk}^{(2)} = N_S \sum_{abc} \left\langle R_{ijk,lmn}(\theta,\psi,\varphi) \right\rangle_{\theta,\varphi,\psi} \beta_{abc}^{(2)}$$

N_s - the surface density of molecules,
(θ,ψ,φ) - Euler angles that define the orientation of the molecular frame relative to the lab frame
R - sixth rank rotational transformation tensor (product of three Euler matrices)

$$\chi_{xxz}^{(2)} = \chi_{yyz}^{(2)} = \frac{1}{2} N_S \beta_{ccc}^{(2)} \left[(1+r)\left\langle \cos\theta \right\rangle - (1-r)\left\langle \cos^3\theta \right\rangle \right]$$

$$\chi_{xzx}^{(2)} = \chi_{zxx}^{(2)} = \chi_{yzy}^{(2)} = \chi_{zyy}^{(2)} = \frac{1}{2} N_S \beta_{ccc}^{(2)} (1-r)\left[\left\langle \cos\theta \right\rangle - \left\langle \cos^3\theta \right\rangle \right]$$

$$\chi_{zzz}^{(2)} = N_S \beta_{ccc}^{(2)} \left[r\left\langle \cos\theta \right\rangle + (1-r)\left\langle \cos^3\theta \right\rangle \right]$$

$$\chi_{xxz}^{(2)} = \chi_{yyz}^{(2)} = -N_S \frac{\beta_{ccc}^{(2)}}{\rho} \left[\left\langle \cos\theta \right\rangle - \left\langle \cos^3\theta \right\rangle \right]$$

$$\chi_{xzx}^{(2)} = \chi_{zxx}^{(2)} = \chi_{yzy}^{(2)} = \chi_{zyy}^{(2)} = N_S \frac{\beta_{ccc}^{(2)}}{\rho} \left\langle \cos^3\theta \right\rangle$$

$$\chi_{zzz}^{(2)} = 2N_S \frac{\beta_{ccc}^{(2)}}{\rho} \left[\left\langle \cos\theta \right\rangle - \left\langle \cos^3\theta \right\rangle \right]$$

Amplitude of C-Si Bend Vibrations

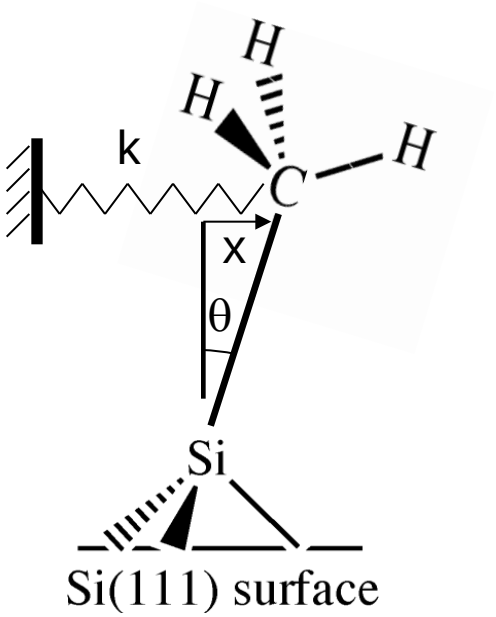

$$\ddot{\theta} = \frac{k \cdot (r_{SiC})^2}{I_{CH3}} \theta$$

$$\omega = \sqrt{\frac{k}{I_{CH3} / r_{SiC}^2}}$$

θ - tilt angle

k – spring constant

ω = 507 cm^{-1} - frequency of vibration

E_0 = ω/2 ~ 250 cm^{-1} vibrational energy

$$E_0 = \frac{k \cdot x^2}{2} \Rightarrow x = \sqrt{\frac{2E_0}{k}} = \sqrt{\frac{2E_0 \cdot r_{SiC}^2}{\omega^2 \cdot I_{CH3}}} \Rightarrow \theta = \arctan\left(\frac{x}{r_{SiC}}\right)$$

x ~ 0.064 A

θ ~ 1.9°

Rotational Dephasing

Classical free-rotor correlation function

$$C(t) = \langle \mu(0) \cdot \mu(t) \rangle = \langle P_1(\cos\theta_t) \rangle = \frac{I_z}{k_B T} \int_0^\infty \cos(\Omega t) \cdot \Omega \cdot \exp\left(-\frac{I_z \Omega^2}{2 k_B T} \right) d\Omega$$

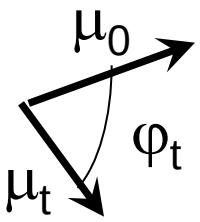

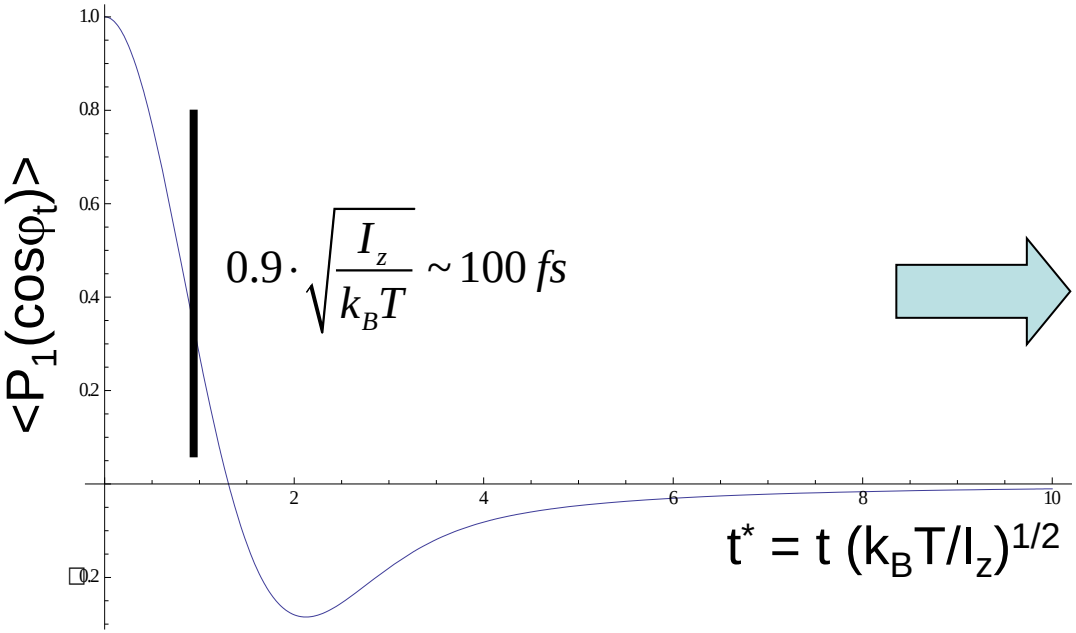

$$0.9 \cdot \sqrt{\frac{I_z}{k_B T}} \sim 100\ fs$$

$\tau_{\text{free rot}}$ ~ 100 fs

Γ_{rot} = 3 cm^{-1}

τ ~ 1.5 ps

Rotational SFG line broadening